THE UNIVERSITY OF CALGARY

# Interactions Between the Inwardly Rectifying Potassium Channels $K_{IR}2.1$ and $K_{IR}3.4$

by

Robert Hay

A THESIS

SUBMITTED TO THE FACULTY OF GRADUATE STUDIES

IN PARTIAL FULFILMENT OF THE REQUIREMENTS FOR THE

DEGREE OF MASTER OF SCIENCE

DEPARTMENT OF CARDIOVASCULAR/RESPIRATORY SCIENCES

CALGARY, ALBERTA

JANUARY, 1998

**Abstract**

*Xenopus* oocytes were injected with inward rectifier potassium channel RNAs for either Kir2.1, Kir3.4, or Kir2.1/Kir3.4. Resulting currents were analyzed with the following properties being measured: current level, extracellular [$K^+$] sensitivity, negative slope conductance, conductance-voltage relationship, and time-dependence of activation. In addition, Kir2.1 was also co-injected with either Kir3.4 or the Kir2.1/Kir3.4 chimeras. Currents fell into one of two categories. Kir2.1-like currents were large and showed sensitivity to $[K^+]_{out}$, negative slope conductance, saturation of conductance at -120 mV, and a time-dependence of activation. Kir3.4-like currents were smaller and showed none of these properties. Analysis of chimeric channels revealed that the N-terminus and pore regions of Kir3.4 were necessary to produce Kir3.4-like properties. Finally, co-expression results suggested that Kir2.1 and Kir3.4 do not interact to form a functional channel and that the pore and C-terminal regions determine the presence or absence of an interaction.

## Table of Contents


Approval Page ..... ii
Abstract ..... iii
Table of Contents ..... iv
List of Tables ..... vi
List of Figures ..... vii
List of Abbreviations ..... viii

**Chapter One: Introduction** ..... 1
A. Inward Rectification and its Role in the Heart ..... 1
B. The Inward Rectifier Superfamily ..... 4
C. Co-expression Studies ..... 11
D. Two Electrode Voltage Clamp and the *Xenopus* Oocyte Model .... 15

**Chapter Two: Materials and Methods** ..... 20
A. Materials ..... 20
i. Molecular Biology ..... 20
ii. Oocyte Isolation and Injection ..... 20
iii. Two-Electrode Voltage Clamp ..... 21
iv. Data Analysis Software ..... 21
B. Methods ..... 22
i. Molecular Biology ..... 22
a. Wild Type Clones ..... 22
b. Chimeric Channel Construction ..... 22
c. cRNA Preparation ..... 25
ii. Oocyte Isolation and Injection ..... 27
iii. Two-Electrode Voltage Clamp ..... 28
C. Data Analysis ..... 29
i. I-V Relationships ..... 29
ii. Absolute Current Levels ..... 30
iii. Conductance Voltage Relationships ..... 30
iv. Time-dependence of Activation ..... 32

**Chapter Three: Study One: Structure-Function Relationships for Kir3.4 and Kir2.1 With Respect to Current Level, $K^+$ Sensitivity, Degree of Inward Rectification, and Time-Dependent Activation** ... 33
A. Objectives and Hypothesis ..... 33
B. Experimental Design Summary ..... 34
C. Results ..... 36
i. Kir3.4 and Kir2.1 Wild Type Currents ..... 36
a. Current Level ..... 36
b. $[K^+]_{out}$ Sensitivity ..... 36

c. Degree of Rectification ..... 37
d. Time-dependence of Activation ..... 40
ii. Kir3.4/Kir2.1 Chimera Currents ..... 42
a. Current Level ..... 42
b. $[K^+]_{out}$ Sensitivity ..... 44
c. Degree of Rectification ..... 45
d. Time-dependence of Activation ..... 46
D. Discussion ..... 47

**Chapter Four: Study Two: Structural Determinants for Interaction Between Kir2.1 and Kir3.4 or Kir2.1/3.4 Chimeric Channels** ..... 63
A. Objectives and Hypothesis ..... 63
B. Experimental Design Summary ..... 64
C. Results ..... 64
i. Co-expression of Kir2.1 With Kir3.4 ..... 64
a. Current Level ..... 64
b. $[K^+]_{out}$ Sensitivity ..... 66
c. Degree of Rectification ..... 67
d. Time-dependence of Activation ..... 68
ii. Co-expression of Kir2.1 With Kir2.1/Kir3.4 Chimeras ..... 69
a. Current Level ..... 69
b. $[K^+]_{out}$ Sensitivity ..... 72
c. Degree of Rectification ..... 73
d. Time-dependence of Activation ..... 77
D. Discussion ..... 77

**Chapter Five: Conclusions** ..... 85

**References** ..... 90

## List of Tables

**Chapter One: Introduction**

1-1 The Inward Rectifier Superfamily ..... 5

**Chapter Two: Materials and Methods**

**Chapter Three: Study One: Structure-Function Relationships for Kir3.4 and Kir2.1 With Respect to Current Level, K+ Sensitivity, Degree of Inward Rectification, and Time-Dependent Activation**

3-1 Summary of results for Study One ..... 49

**Chapter Four: Study Two: Structural Determinants for Interaction Between Kir2.1 and Kir3.4 or Kir2.1/Kir3.4 Chimeric Channels**

4-1 Summary of results for Study Two ..... 78

## List of Figures

### Chapter One: Introduction


1-1 Typical Steady-State Current-Voltage Relationships for Delayed and Inward Rectifier Currents ..... 2
1-2 Predicted Membrane Topology for Inward Rectifiers ..... 7
1-3 Conventional Two-Electrode Voltage Clamp ..... 18


### Chapter Two: Materials and Methods


2-1 Schematic Representation of Chimeric Channels ..... 23


### Chapter Three: Study One: Structure-Function Relationships for Kir3.4 and Kir2.1 With Respect to Current Level, K+ Sensitivity, Degree of Inward Rectification, and Time-Dependent Activation


3-1 Current Level Comparison for Kir2.1 and Kir3.4 ..... 37
3-2 Outward Current Comparison for Kir2.1 and Kir3.4 ..... 38
3-3 Conductance-Voltage Relationships for Kir2.1 and Kir3.4 ..... 39
3-4 Boltzmann Fits to gKrel-V Relationships for Kir2.1 and Kir3.4 ..... 40
3-5 Time-Dependent Activation for Kir2.1 and Kir3.4 ..... 41
3-6 Current Level Comparison for ICI, CCI, and CII ..... 43
3-7 Outward Current Comparisons for ICI, CCI, and CII ..... 44
3-8 Conductance-Voltage Relationships for ICI, CCI, and CII ..... 46
3-9 Boltzmann Fits for ICI, CCI, and CII ..... 47
3-10 Time-Dependence of Activation for ICI, CCI, and CII ..... 48


### Chapter Four: Study Two: Structural Determinants for Interaction Between Kir2.1 and Kir3.4 or Kir2.1/Kir3.4 Chimeric Channels


4-1 Current Level for Kir2.1/Kir3.4 ..... 65
4-2 Outward Current Comparison for Kir2.1/Kir3.4 ..... 66
4-3 Conductance-Voltage Relationships for Kir2.1/Kir3.4 ..... 68
4-4 Time-Dependent Activation for Kir2.1/Kir3.4 ..... 69
4-5 Representative Kir2.1/Chimera Co-expression Currents ..... 70
4-6 Current Levels for Kir2.1/Chimera Co-expression Currents..... 71
4-7 Outward Current Comparisons for Kir2.1/Chimera Co-expression Currents ..... 73
4-8 Conductance-Voltage Relationships for Kir2.1/Chimera Co-expression Currents ..... 74
4-9 Boltzmann Fits for Kir2.1/Chimera Co-expression Currents ..... 75
4-10 Time-Dependence Activation for Kir2.1/Chimera Co-expression Currents 76

## List of Abbreviations

| | |
|---|---|
| SA Node | sino-atrial Node |
| AV Node | atrio-ventricular Node |
| Kir | potassium inward rectifier |
| SUR | sulfonyurea receptor |
| RNA | ribonucleic acid |
| DNA | deoxyribonucleic acid |
| PCR | polymerase chain reaction |
| BSA | bovine serum albumin |
| ANOVA | analysis of variance |
| SEM | standard error of the mean |
| ATP | adenosine triphosphate |

# Chapter One: Introduction

## A. Inward Rectification and its Role in the Heart

Originally described by Katz as "anomalous rectification", inwardly rectifying potassium channels have an asymmetrical conductance that is characterized by larger inward than outward current [Katz, 1949]. The anomaly that Katz was referring to was the fact that inward conductance increases with hyperpolarization and outward conductance decreases with depolarization, an effect that is opposite to the effect of voltage on previously described delayed rectifier potassium channels (Figure 1-1) [Katz, 1949; Vandenberg, 1995]. In cardiac cells, the inward rectification feature plays an extremely important role in several potassium currents including the classical inward rectifier current $I_{K1}$ [Vandenberg, 1995; Isenberg, 1976; Sakmann and Trube, 1984; Shimoni *et al.*, 1992], the muscarinic G-protein linked $I_{KACh}$ current [Vandenberg, 1985; Heidbüchel *et al.*, 1987; Heidbüchel *et al.*, 1990], and finally, the ATP-sensitive current $I_{KATP}$ [Vandenberg, 1995; Ashcroft, 1988; Noma, 1983]. Generally speaking, inward rectifiers play an important role in determining the resting membrane potential which varies among cells that play different physiological roles. The requirements for a particular cell type with respect to membrane potential dictate the numbers and types of inward rectifiers present, each of which is suited to their specific role according to their degree of rectification and modulation by neurotransmitters and intracellular signals.

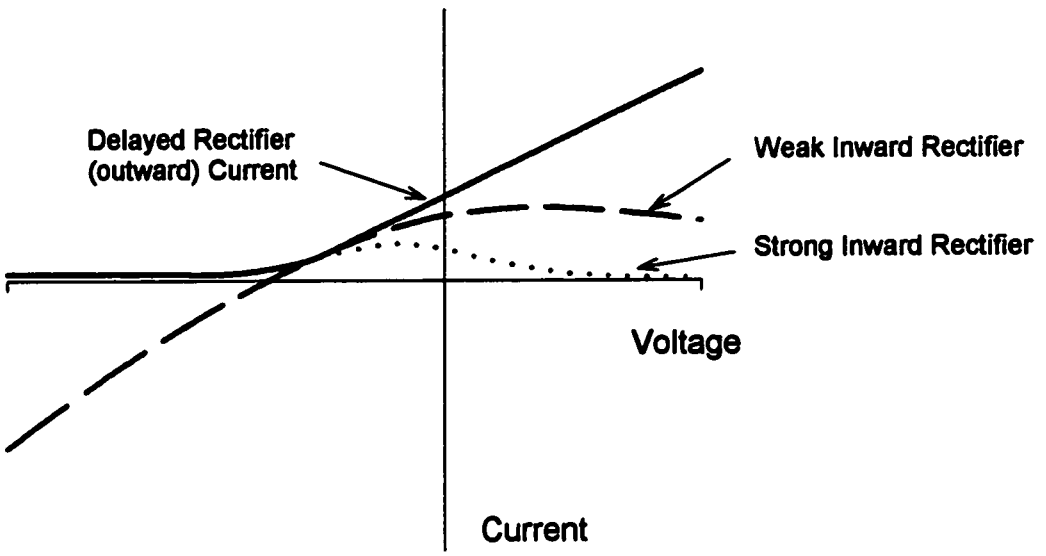


**Figure 1-1. Typical Steady-State Current-Voltage Relationships for Delayed and Inward Rectifier Currents.** Typical delayed rectifier current is shown as solid line. A typical strong inward rectifier current is shown as the dotted line. A typical weak inward rectifier current is shown as the dashed line.

The inward rectifier $I_{K1}$ plays a predominant role in maintaining resting membrane potential and contributes to the final phase of repolarization in the cardiac action potential [Shimoni *et al.*, 1992; Mazzanti and DeFelice, 1988; Ibarra *et al.*, 1991]. It plays its most influential role in ventricular cells but is also present in atrial and Purkinje cells but it is absent in the pacemaking cells of the SA and AV nodes [Hume and Uehara, 1985; Giles and Imaizumi, 1988; Irisawa *et al.*, 1987]. An important feature of $I_{K1}$ is its strong inward rectification that is represented by a lack of any substantial current 20 mV positive to the reversal potential. As a result, $I_{K1}$ is perfectly suited in its role in stabilizing the membrane potential at or around $E_K$ and allows for long lasting depolarizations

with little metabolic expense to the cell due to loss of intracellular $K^+$ [Hille, 1992]. The highly negative resting membrane potential and long action potential duration of ventricular cells can be attributed to the high density of $I_{K1}$ channels present in these cells [Vandenberg, 1995].

In contrast to ventricular cells, nodal cells display a more positive membrane potential which is partially due to the absence of $I_{K1}$ [Giles and Imaizumi, 1988]. The dominant inward rectifier in nodal cells is the G-protein gated $I_{KACh}$. Its more modest rectification and modulation by vagal stimulation allows for more flexibility in membrane potential which is a necessity in pacemaking cells that determine heart rate. Atrial cells display a resting membrane potential that is in between that of nodal and ventricular cells [Giles and Imaizumi, 1988]. This is due to presence of both $I_{KACh}$ and $I_{K1}$. In addition to $I_{K1}$ and $I_{KACh}$, cells throughout the heart show an ATP sensitive current $I_{KATP}$ that only plays a role in time of ischaemia when intracellular ATP levels drop. Therefore, the ATP dependent gating of this channel allows it to open during ischaemia so that action potential duration is shortened. Specifically, a shorter plateau phase reduces the amount of $Ca^{++}$ influx due to the L-type calcium channel [Cole *et al.*, 1991; McPherson *et al.*, 1993; Cole and Aeillo, 1994]. The end result is that less ATP is consumed for pumping $Ca^{++}$ back into the sarcoplasmic reticulum.

In short, the pattern of distribution for inward rectifiers is dictated by the differences in membrane potential requirements of specific cell types. Cells

needing a well defined and stable resting membrane potential require a strong inward rectifier, while cells that require more flexibility in their resting potential utilize a moderate inward rectifier that can be modulated by the autonomic nervous system, and finally, all cells require an inward rectifier that can offer protection during times of ischaemia.

## B. The Inward Rectifier Superfamily

Originally, studies on inward rectifiers focused on defining the electrophysiological characteristics for each current. For example, studies on the classical inward rectifier $I_{K1}$ demonstrated that it is $K^+$ selective, can be blocked by external $Ba^{++}$ and $Cs^{++}$, shows strong inward rectification with a dependence of rectification on external $K^+$, has a square root dependence of conductance on external $K^+$, and finally it shows an inactivation dependence on external $Na^+$ [Vandenberg, 1995; Isenberg, 1976; Sakmann and Trube, 1984; DiFrancesco *et al.*, 1984; Vandenberg, 1987; Biermans *et al.*, 1987]. However, recent cloning of genes that encode inward rectifier potassium channels have shifted the focus towards studying the structure-function relationships of a particular channel. Multiple clones have been isolated leading to the development of a standardized nomenclature which divides inward rectifiers into 6 subfamilies, based upon sequence similarities, that together form the Kir ($K^+$ Inward Rectifier) Superfamily (Table 1-1) [Doupnik *et al.*, 1995; Nichols and Lopatin, 1997]. The IRK1 gene encodes the $I_{K1}$ channel and is a

**Table 1-1. The Inward Rectifier Superfamily.**

| Subfamily | Number of Members | Rectification | Distribution | Features |
|---|---|---|---|---|
| 1.0 | 1 (Kir 1.1) | weak | kidney, brain | multiple splice variants |
| 2.0 | 3 (Kir2.1-2.3) | strong | heart, nervous system | indistinguishable from native $i_{K1}$ |
| 3.0 | 4 (Kir3.1-3.4) | strong | heart, brain, endocrine system | G-protein regulated |
| 4.0 | 1 (Kir4.1) | weak | brain | co-assembles with Kir5.1 |
| 5.0 | 1 (Kir5.1) | does not express | brain | co-assembles with Kir4.1 |
| 6.0 | 2 (Kir6.1-6.2) | strong | ubiquitous | co-assembles with sulfonyurea (SUR) receptor |

member of the Kir2.0 subfamily and will be referred to as Kir2.1 [Kubo *et al.*, 1993]. The GIRK1 and CIR genes together form the $I_{KACh}$ channel and are members of the Kir3.0 subfamily and will be referred to as Kir3.1 and Kir3.4 respectively [Krapivinsky *et al.*, 1995]. Finally the Kir6.1 gene, of the Kir6.0 subfamily, along with the SUR receptor gene assemble to form $I_{KATP}$ [Inagaki *et al.*, 1995a; Inagaki *et al.*, 1995b]

Since the first clone was isolated a great deal of information has been accumulated that has helped answer questions regarding the general structure

of inward rectifiers and what molecular determinants are involved in the physiological properties of inward rectifiers. Based on nucleotide sequences and hydrophobicity plots, a structural model has been made suggesting that inward rectifiers are membrane proteins characterized by two membrane spanning domains, a putative pore region, two minor extracellular loops, and intracellular N- and C-terminal domains (Figure 1-2) [Doupnik *et al.*, 1995; Kubo *et al.*, 1993a; Kubo *et al.*, 1993b; Ashford *et al.*, 1994; Krapivinsky *et al.*, 1995; Inagaki *et al.*, 1995; Ho *et al.*, 1993]. Evidence that the putative pore region forms part of the $K^+$ selective pore comes from the fact that there is extensive sequence similarity with the well studied P-region (H5) of voltage-gated (Kv) channels [Jan and Jan, 1992; Brown, 1993; Pongs, 1993]. There is also some limited sequence similarity between the membrane spanning domains (M1, M2) of the inward rectifiers with the S5 and S6 membrane spanning domains of the Kv channel family. In short, the membrane topology of the inward rectifiers resembles the S5, H5, and S6 segments of the voltage gated family of $K^+$ channels, but form their own family based on different structural and electrophysiological properties.

Structure-function studies have determined that the $K^+$ selectivity property is due to a GYG signature sequence in the pore region that when mutated leads to a non-selective cationic pore [Slesinger *et al.*, 1996]. Also, evidence presented in another study by the Jan laboratory suggested that two oppositely charged residues (Glu-138 and Arg-148) in the H5 region of the Kir2.1 clone

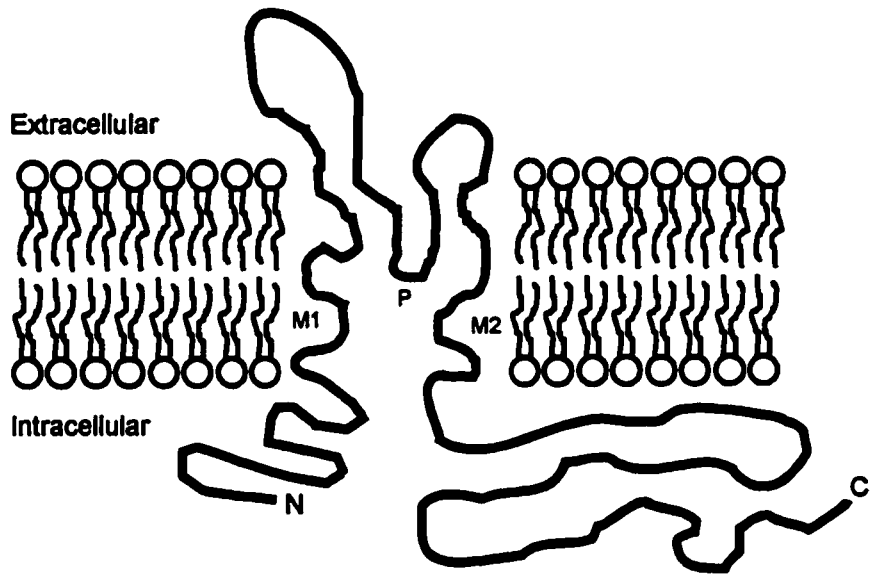


**Figure 1-2. Predicted Membrane Topology for Inward Rectifers.** Intracellular N- and C-terminal domains are flanked by two membrane spanning domains, M1 and M2, plus two minor extracellular loops, and the putative pore region, P.

form an exposed salt bridge that is necessary for maintenance of the structural stability of the selectivity filter [Yang *et al.*, 1997]. Any mutation or alteration of these residues dramatically alters permeation and ion selectivity. Other studies related to the conductance properties of inward rectification have revolved around studying the property of inward rectification itself. Of course it was already known that inward rectification was due to voltage and time-dependent block of the pore by intracellular $Mg^{++}$ and what Nichols termed "intrinsic rectifying factors", now known to be polyamines [Matsuda, 1991; Ficker *et al.*, 1994; Lopatin *et al.*, 1994; Fakler *et al.*, 1994]. The question was why are some

currents more strongly rectified than others? Heterologous expression of inward rectifier clones and site directed mutagenesis revealed the importance of a single amino acid (172) in the M2 region that was involved in the voltage-dependent block by $Mg^{++}$ [Lu and MacKinnon, 1994]. Strong inward rectifiers like Kir2.1 present a negative charge (D172) at that position, whereas weak inward rectifiers like Kir1.1 contain a neutral residue (N172) [Doupnik *et al.*, 1995; Ficker *et al.*, 1994; Lu and MacKinnon, 1994; Wible *et al.*, 1994; Stanfield *et al.*, 1994]. Also, a study by Taglialatela and co-workers revealed that there is an additional site in the C-terminus that is also important for rectification: Mutation of E224 to a G, S, or Q significantly reduced rectification by decreasing block by internal $Mg^{++}$ and polyamines [Taglialatela *et al.*, 1995]. These results suggest that the 172 and 224 positions contribute to the formation of a binding site for $Mg^{++}$ and polyamines, and therefore, the amino acids present at those positions play an important role in determining the degree of rectification.

One of the other areas that has received a considerable amount of attention is defining the determinants for G-protein regulation. Dascal and co-workers demonstrated that the Kir3.1 channel is inhibited by blockage of the channel by the C-terminal tail in a manner that was analogous to the N-terminal "Shaker ball" peptide of certain rapidly inactivating Shaker-type K channels [Dascal *et al.*, 1995]. Also, studies by Kunkel and Peralta [Kunkel and Peralta, 1995] and the Jan laboratory [Huang *et al.*, 1997] have suggested that binding of $G\beta\gamma$, which is involved in activation of the channel, is confined to N- and C-

terminal regions that are adjacent to the putative channel pore. These results suggest that activation of the channel results when competing Gβγ remove the blocking C-terminus and allow for permeation. The important thing to note here is that the Kir3.0 subfamily is unique in its capacity to be regulated by G-proteins. Members of this subfamily are therefore subjected, in addition to inactivation by rectification, an inactivation mechanism that is relieved by G-proteins.

To summarize, a large number of studies have focused on and provided valuable insight into the properties of $K^+$ selectivity, inward rectification, and G-protein modulation. However, the majority of these studies have neglected analysis of the outward current that flows through inward rectifiers. Indeed this is somewhat puzzling in that it is the outward portion that plays the more important physiological role. As already mentioned, only the outward portion of the $I_{K1}$ current plays an important role in the final phase of repolarization of the cardiac action potential. Actually, the characteristic current-voltage relationship of the $I_{K1}$ current displays a prominent region of negative slope in its outward portion. The effect of this feature is that as cells begin to repolarize the outward current actually increases, promoting a rapid repolarization. The Kir2.1 clone, which is thought to encode the $I_{K1}$ channel, shows a definite region of negative slope when expressed in *Xenopus* oocytes. This contrasts with another clone, Kir3.4, that we have isolated from a mouse atrial tumor cell line which shows no evidence of negative slope. The focus of this thesis is on these two clones,

Kir2.1 and Kir3.4, both of which differ dramatically not only in their outward currents, but also with respect to degree of rectification, sensitivity to extracellular $K^+$, time-dependence of activation, and level of expression.

The **objective** of Study One was to broadly define the structural regions present in Kir3.4 or Kir2.1 that are important in determining current level, sensitivity to extracellular $K^+$, degree of rectification, and time-dependence of activation. The reason for doing this experiment is that studies involving individually expressed Kir3.4 channels are limited and as a result it has not been thoroughly analyzed [Iizuka *et al.*, 1995; Chan *et al.*, 1996]. The reason for using Kir2.1 in these experiments is that it provides a sharp contrast with which Kir3.4 can be compared. Kir2.1 shows a high current level, an increase in outward current with an increase in extracellular $[K^+]$, strong inward rectification with a negative slope conductance, and a time-dependence of activation. Kir3.4 shows a low current level, no sensitivity to extracellular $[K^+]$, weak inward rectification with no negative slope conductance, and no time-dependent activation. Defining the structural regions involved in displaying these properties was accomplished by constructing chimeric channels with Kir2.1 and Kir3.4 that divides the channels into 3 regions: the N-terminal, pore, and C-terminal regions.

The **hypothesis** is that with respect to current level the intracellular N- and C-terminal regions will play an important role for Kir3.4 while for Kir2.1 the C-terminus and pore will be more important. The prediction for Kir3.4 is based on previous studies that have already been discussed in this introduction with regards to G-protein regulation of the Kir3.0 subfamily. The prediction for Kir2.1 is based on a study by the Jan laboratory regarding assembly of inward rectifiers whereby they concluded that the M2 and proximal C-terminus are important for homotypic interactions between identical subunits [Tinker *et al.*, 1996]. For both Kir2.1 and Kir3.4 the properties of sensitivity to extracellular $K^+$, degree of rectification, and time-dependent activation will be determined by the pore and C-terminal regions. All of these properties are directly related to the mechanism of rectification, and therefore, this prediction is based on the previously mentioned studies that identified important sites in both the M2 and C-terminal regions.

## C. Co-expression Studies

The demonstration that the subunit stoichiometry for inward rectifiers is four [Yang *et al.*, 1995] came as no real surprise since the distantly related voltage-gated channels were also shown to be tetramers [Liman *et al.*, 1992; MacKinnon, 1991]. Indeed, this structural plan mimics the design of the principle pore-forming subunit for monomeric voltage gated $Na^+$ and $Ca^{++}$ channels that contain four homologous internal repeats [Yang *et al.*, 1995; Noda

*et al.*, 1984; Tanabe, 1987]. The tetrameric nature for inward rectifiers leads to the possibility of heteromultimerization which is now known to occur. When clones for inward rectifiers were first being isolated Ashcroft and co-workers presented evidence that they had isolated a clone that encoded the $I_{KATP}$ channel [Ashcroft *et al.*, 1994]. However, conflicting evidence presented by Clapham's group suggested that this clone did not contribute to $I_{KATP}$, but in fact combined with GIRK1 or Kir3.1 to form the $I_{KACh}$ channel [Krapivinsky *et al.*, 1995a, Krapivinsky *et al.*, 1995b]. The evidence they presented involved the use of antibodies directed to Kir3.1 that could co-precipitate an unknown 45 kDa protein that turned out to be identical to the protein sequence for the clone isolated by Ashcroft *et al* [1994]. This clone was then termed the cardiac inward rectifier or CIR, but is now referred to as Kir3.4. Heterologous co-expression of both Kir3.1 and Kir3.4 resulted in the formation of channels that were G-protein gated and displayed single channel kinetics that more closely resembled the native atrial $I_{KACh}$ channel than either homomeric channel [Krapivinsky *et al.*, 1995a]. This synergistic effect was the first demonstration that inward rectifiers could indeed be composed of more than one type of subunit. In fact, Kir3.1 does not form functional channels on its own, although current can be seen when injected into *Xenopus* oocytes due to the presence of a low level of an endogenous inward rectifier, XIR (*Xenopus* inward rectifier), that is highly homologous to the Kir3.4 clone [Hedin *et al.*, 1996]. These results suggested

that inward rectifying currents present in any cell may be a composite of homo- and heteromultimers.

The synergistic effect seen with co-expression of Kir3.1 and Kir3.4 contrasts with results reported in other studies involving the co-expression of one inward rectifier with another. A negative interaction was seen when Kir3.4 was co-expressed with either Kir2.2 or Kir4.1 to the point that these currents were almost completely abolished [Kunkel and Peralta, 1995; Tucker *et al.*, 1996]. Actually, some studies have gone so far as to co-express inward rectifiers with members of the voltage-gated family, again with negative results [Tygat *et al.*, 1996]. To date positive interactions have only been seen when members of the same subfamily are co-expressed.

Since the time it was shown that inward rectifiers are tetramers and that different subunits can to some extent interact, there have been numerous studies that have attempted to define which structural regions are involved in assembly of both homomultimeric and heteromultimeric channels. However, there seems to be contradicting results in terms of which regions play what roles for co-assembly and for the incompatibility between subunits from different subfamilies. Using dominant-negative chimeras constructed with Kir2.3 and Kir3.2, Fink and co-workers provided evidence that the N-terminal region plays a crucial role in the assembly of IRK type subunits (Kir2.0 subfamily) into functional channels [Fink *et al.*, 1996]. Another study by Tucker and co-workers also used dominant-negative chimeras, this time Kir4.1 and Kir3.4, to show that

the transmembrane domains are the structural elements necessary for an inhibitory effect of Kir3.4 on Kir4.1 [Tucker *et al.*, 1996]. Finally, biochemical and electrophysiological methods were employed in the Jan laboratory to study chimeras constructed from Kir2.1, Kir2.2, Kir2.3, Kir1.1 and Kir6.1. The data which these investigators obtained suggest that the proximal C-terminus and the M2 transmembrane segment are important for both homomultimeric assembly and for the incompatibility between different subfamilies [Tinker *et al.*, 1996]. In short, there is evidence that either the N-terminus, transmembrane domains, or proximal C-terminus and M2 together play the most important roles in assembly. It is possible that the contradictory results are a manifestation of the varying subunits used in each particular study, and that interactions between different subunits and the regions involved are case specific.

The **objective** for Study Two was to co-express Kir2.1 and Kir3.4 in *Xenopus* oocytes and determine if there is any interaction between them. Also, Kir2.1 was co-expressed with the chimeric channels used in Study One to determine which structural regions are necessary for the presence or lack of any interaction described above. The rationale for co-expressing Kir2.1 with Kir3.4 is that both of these clones are expressed in the same areas of the heart [Kubo *et al.*, 1993; Iizuka *et al.*, 1995], and therefore any interaction may be physiologically relevant.

The **hypothesis** is that since these clones are from different subfamilies, there will be either no interaction or a negative interaction. This prediction is based on the co-expression studies mentioned previously. The structural regions that confer any interaction or incompatibility will be restricted to the M2 containing pore region and the C-terminus. The reason for this prediction is based on the Tinker *et al.* [1996] study involving the assembly of inward rectifiers. That study did not involve the use of Kir3.4, but did concern Kir2.1, and therefore, the results in this study are expected to parallel the results obtained by the Jan laboratory.

### D. Two Electrode Voltage Clamp and The *Xenopus* Oocyte Model

The model system that was used to express the wild type and chimeric channels mentioned above was the *Xenopus* oocyte. The main reason for using this model was that the two-electrode voltage clamp setup required for measuring currents in injected oocytes was firmly established in the lab when these experiments were being started. In fact, both the Kir2.1 and Kir3.4 clones had already been expressed and current recordings were obtained which made these studies extremely feasible. However, there are both advantages and disadvantages to this model which I will now describe in some detail.

What is a *Xenopus* oocyte? A *Xenopus* oocyte is an egg precursor that when hormonally stimulated can pass through the frog's oviduct to become an egg which can then be fertilized to become a frog. Oocytes are stored in the

abdominal cavity in clumps called ovarian lobes which also contain connective tissue, blood vessels, and follicle cells. Oocytes pass through six developmental stages termed stage I to VI, where stages V and VI are most commonly used for electrophysiology. They are large cells with a diameter of approximately 1-1.2 mm and are surrounded by a vitelline membrane and a follicle cell layer. The presence of the vitelline membrane provides its spherical shape and more importantly structural stability so that exogenous mRNA can be injected into the cytoplasm for expression of a desired protein, in this case, inward rectifier potassium channels. The currents that are produced by the foreign protein can be measured using two-electrode voltage clamp methodology [Sherman-Gold, 1993; Rudy and Iverson, 1992] (Figure 1-3). In this method, one intracellular electrode records the actual intracellular potential while the second intracellular electrode is used to pass current so that a desired potential can be maintained. This is achieved by a feedback circuit whereby the difference in potential between the bath and the voltage sensing electrode ($V_m$) is compared to the command potential ($V_{cmd}$), with any difference being negated by injecting into or withdrawing charge from the oocyte through the current passing electrode. The injected current flows to ground through the bath ground electrode.

The disadvantages of using this model involves the size of the oocyte and the presence of follicular cells. The large size of an oocyte gives a corresponding surface area on the order of $10^6$ $\mu m^2$, and may be even higher considering invagination of the cell membrane that may double or triple this

number. This is an enormous amount of surface area that needs to be charged when clamping the cell. In cases where the current of interest is large and activates rapidly there may be inadequate control of the voltage during the initial phases of channel activation. The response time ($\tau$) of a voltage clamp to a step voltage change is,

$$\tau = R_I C_M / A \quad (1)$$

where $R_I$ is the resistance of the current passing electrode, $C_M$ is the membrane capacitance, and A is the gain of the command amplifier [Sherman-Gold, 1993]. With this in mind, the response time can be kept to a minimum by using a current passing electrode with a small resistance and setting the microelectrode amplifier to maximal gain without losing stability. Also, to obtain the fastest response, the electrodes are shielded by placing a grounded metal sheet between them to reduce capacitive coupling. Finally, smaller oocytes (stage III-IV) may be used to lower response time. These precautions are necessary for rapidly activating currents so that resulting current recordings will minimize a large capacitive transient that may mask events that occur early in a voltage step. Follicular cells are electrically coupled to each other and the oocyte through gap junctions and therefore electrical events in the follicle are detected in the oocyte. Recording from the oocyte means that you are also recording from the follicle. Also, impalement of the oocyte with an injecting pipette or microelectrode can be difficult if the follicle is left on. Removal of the follicular layer involves treatment with collagenase followed by manual removal

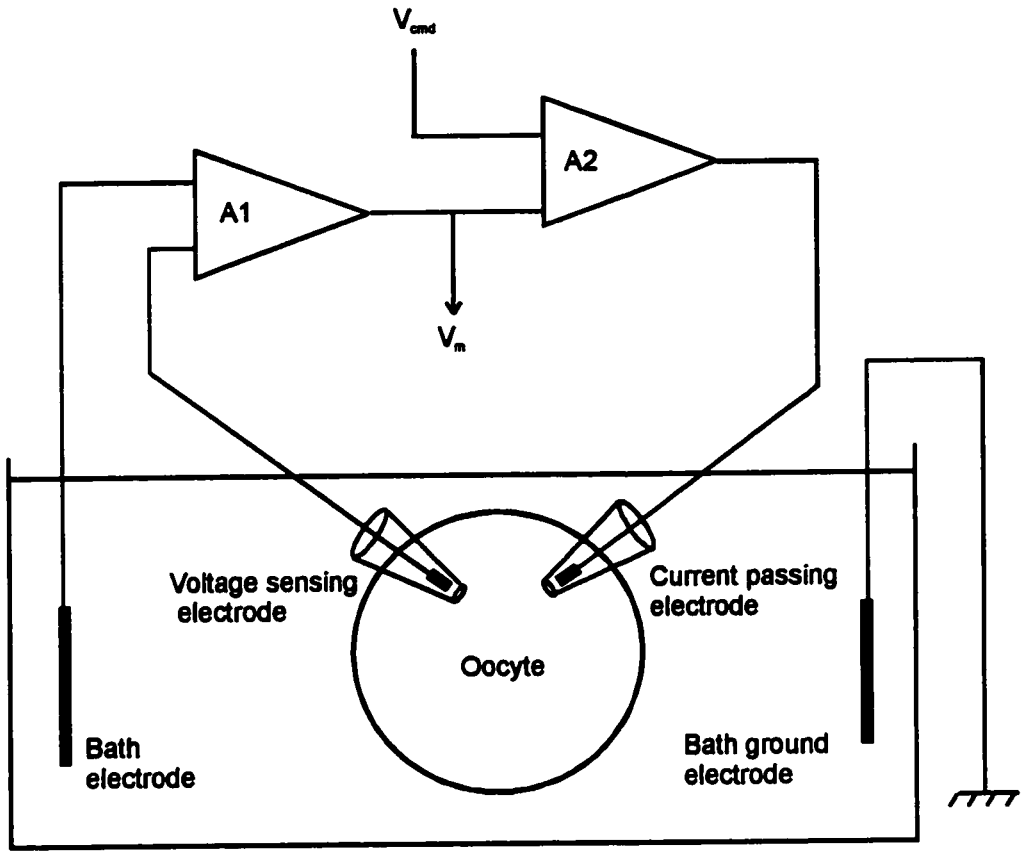


**Figure 1-3. Conventional Two-Electrode Voltage Clamp.** The difference in potential between the bath and voltage sensing electrodes ($V_m$) becomes the output of the A1 amplifier. $V_m$ is compared to the command potential, $V_{cmd}$, by the A2 amplifier which passes current into the oocyte in order to minimize the difference between $V_m$ and $V_{cmd}$.

of individual de-folliculated oocytes. Not only is this procedure time-consuming but it imparts a degree of damage that compromises the quality of the oocyte. One final disadvantage to the use of *Xenopus* oocytes is the large batch to batch variability in the size of currents produced from a single batch of *in vitro* transcribed cRNA.

The advantages to this model are simple. First, the large size and durability of oocytes makes injection of exogenous RNA possible without

damaging or disrupting the overall stability of the cell. Second, the *Xenopus* oocyte has very few endogenous channels that can make measuring the current of interest more complicated. There are two currents of importance for this study that include a calcium-activated chloride current and an endogenous inward rectifier current. The chloride current can be blocked by niflumic acid and the inward rectifier current although important is at such a low density that it was not detected in our studies.

# Chapter Two: Materials and Methods

## A. Materials

### i. Molecular Biology

* Mouse Kir2.1 and Kir3.4 clones
* Restriction enzymes: Bam*HI*, Bgl*II*, Hind*III*, Nco*I*, Nsp*V*, Sal*I*, Sac*I*, Sca*I*, Sma*I*, Sph*I*, Stu*I*, Xba*I*
* *Taq* DNA Polymerase
* PCR primers: CIRSal*I*-5', CIRNsp*V*-3', CIRSal*I*-3', CIRNsp*V*-5', CIRNco*I*
* T4 DNA Ligase
* Thermosequenase DNA Sequencing Kit (Amersham)
* mESSAGE mACHINE™ in vitro RNA transcription Kit (Ambion)
* pBluescript KS+ cloning vector (Stratagene)
* pGEX cloning vector: pGEM -3Zf(-) cloning vector (Promega) plus 5' untranslated region of the *Xenopus* β-globin gene
* Ribosomal RNA standard

### ii. Oocyte Isolation and Injection

* Adult female frogs, *Xenopus laevis* (Nasco)
* Sigma Chemicals: MS-222 (Tricaine), collagenase TypeIA, bovine serum albumin (BSA), penicillin/streptomycin, NaCl, KCl, $MgCl_2$, $MgSO_4$, $Ca(NO_3)_2$, $CaCl_2$, $NaHCO_3$, theophylline, sodium pyruvate, Hepes

* gentamicin sulphate (Schering)
* Nanoject Automatic Injector (Drummond)
* 3½" capillary tubes for injection (Drummond)
* P87 Pipette puller (Sutter Instruments)
* Low Temperature Incubator (VWR)

### iii. Two-Electrode Voltage Clamp

* Geneclamp 500 Amplifier (Axon Instruments Inc.)
* Digidata 1200 A/D converter (Axon Instruments Inc.)
* Oscilloscope V-134 (Hitachi)
* Computer with 486 (or higher) microprocessor
* pClamp 6.0.1 Data acquisition software
* glass filament, thin wall, 1.5 mm x 1.12 mM, 6" recording pipettes (A-M Systems, Inc.)
* P87 Pipette Puller (Sutter Instruments)
* Sigma chemicals: NaCl, KCl, $CaCl_2$, BaCl, Hepes, niflumic acid

### iv. Data Analysis Software

* Sigmaplot 4.0 (Jandel Scientific)
* SigmaStat 2.0 (Jandel Scientific)
* pClamp 6.0.1 Data Acquisition and Analysis (Axon Instruments Inc.)

## B. Methods

### i. Molecular Biology

#### a. Wild Type Clones

The mouse Kir2.1 clone was a gift from the Jans who isolated it from a J774 mouse macrophage cell line by expression cloning, Genbank accession number X73052 [Kubo *et al.*, 1993a]. The original clone received was digested with Hind*III* and Stu*I* and then subcloned into pBluescript KS+ (Stratagene) cut with Hind*III* and Sma*I*. The mouse Kir3.4 was cloned previously in our lab by Dr. J. Lees-Miller by PCR and homology screening of a mouse AT1 (atrial tumor) cell cDNA library. A full length clone was digested with Bgl*II* and Xba*I* and then subcloned into a modified pGEM -3Zf(-) (Promega) vector cut with Bam*HI* and Xba*I*. The modified pGEM -3Zf(-) vector, called pGEX, contained an extra 50 base pairs from the 5' untranslated region of the *Xenopus* β-globin gene.

#### b. Chimeric Channel Construction

A schematic drawing illustrating the six chimeras produced in this study is shown in Figure 2-1. Construction of the chimeric channels revolved around separating each clone into three distinct regions according to amino acid sequence. The cut sites used were chosen due to the position of two convenient restriction sites present in the Kir2.1 clone. These include a Sal*I* site approximately 8 amino acids upstream from the border of the N-terminal and M1 domains and a Nsp*V* site approximately 30 amino acids downstream from the

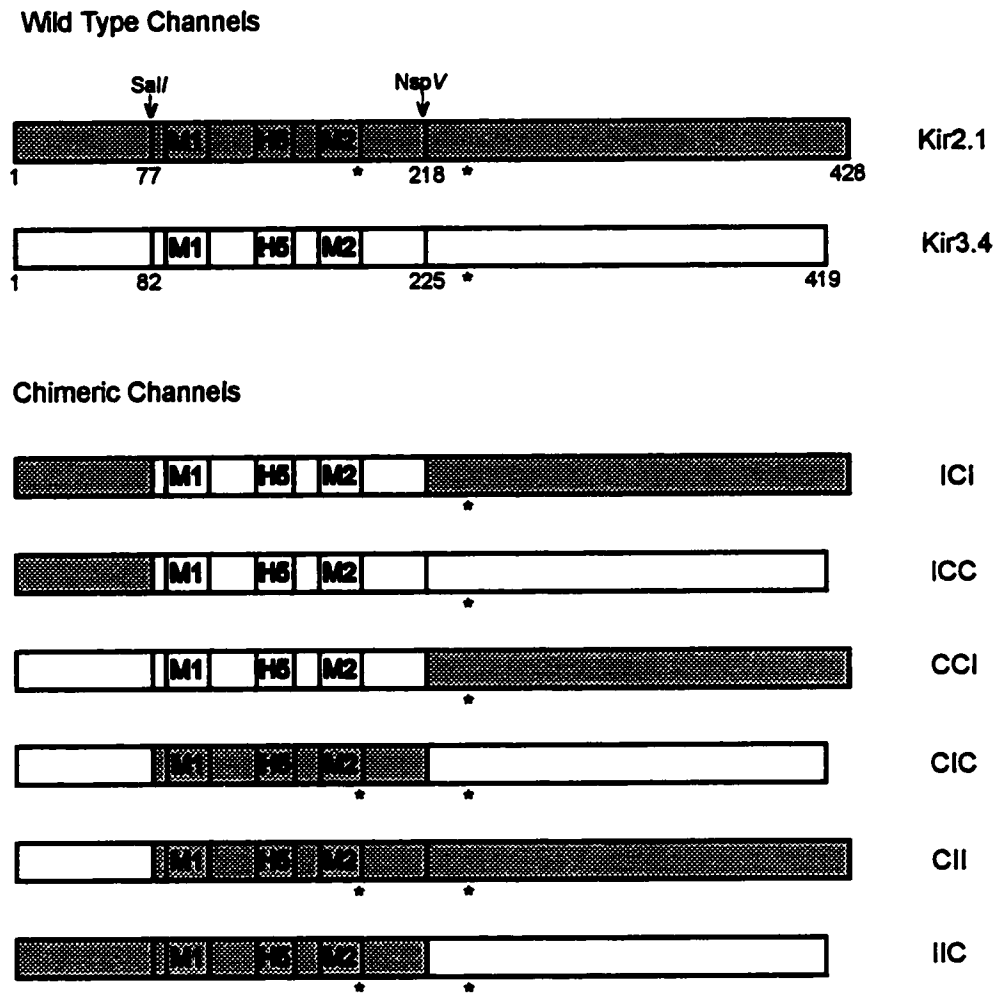


**Figure 2-1. Schematic Representation of Chimeric Channels.** Kir2.1 clone contained convenient restriction sites, SalI and Nsp*V*, that separate the clone into 3 distinct regions. The N-terminal region, the pore region, and the C-terminal region. Position of SalI and Nsp*V* sites are shown. Also shown are the predicted membrane spanning domains, M1 and M2, which flank the putative pore region, H5. Asterisks indicate the negative charges for D172 and E224 for Kir2.1 and the analogous sites in Kir3.4, that have been shown to be important for inward rectification.

M2 domain. The Nsp*V* site was ideal in that it separated both the two important sites for rectification (172 and 224) and the two important regions for assembly of Kir2.1 (M2 and proximal C-terminus 230-300 amino acids). This conveniently

separated the clones into the N-terminal, pore, and C-terminal regions. The N-terminal region contained amino acids 1-77 for Kir2.1, and 1-82 for Kir3.4. The pore region includes 78-218 or 83-225 for Kir2.1 and Kir3.4 respectively. Finally, the C-terminal regions include 219-428 for Kir2.1 and 226-419 for Kir3.4 (Figure 2-1). The nomenclature for the six chimeras is based on the original names for Kir2.1 and Kir3.4, which were IRK1 and CIR respectively. The letter I designates IRK1 and C designates CIR. For example, the ICI chimera contains the N- and C-terminal regions of Kir2.1 (IRK1) and the pore region of Kir3.4 (CIR).

The strategy for construction of the three chimeras that contain the Kir3.4 pore region involved several steps. Step one involved PCR with the Kir3.4 clone using primers (CIRSal*I*-5', CIRNsp*V*-3') that incorporated the Sal*I* and Nsp*V* sites that are present in Kir2.1. The resulting PCR product was digested with Sal*I* and Nsp*V* and subcloned into Kir2.1 which had the Sal*I*/Nsp*V* fragment removed forming the ICI chimera. The ICC chimera was obtained by digesting the ICI chimera with Nco*I* and Xba*I* and isolating the vector into which the Nco*I*/Xba*I* fragment from Kir3.4 was inserted. The CCI chimera was obtained by inserting the Bam*HI* fragment from the ICI chimera into Kir3.4 which was similarly cut with Bam*HI*.

The strategy for construction of the chimeras that contain the Kir2.1 pore also involved several steps. The first step involved PCR with Kir3.4 using primers (CIRNco*I*, CIRSal*I*-3') that include a mutant Nco*I* site at the start ATG

codon and the *SalI* mutation at the end of the N-terminal region. This PCR product was isolated and then digested with *NcoI* and *SalI* and finally inserted into the pGEX vector cut with *NcoI* and *SalI*. The CII chimera was then created by cutting this construct with *SalI* and *SacI* and inserting the Kir2.1 *SalI*/*SacI* fragment. CII was digested with Nsp*V* and *XbaI* so that the Nsp*V*/*XbaI* fragment from Kir3.4 could be inserted to form an intermediate construct, called CIC-Nsp*V*. The next step involved PCR with Kir3.4 using a primer (CIRNsp*V*-5') that incorporated the desired NspV site. The PCR product was digested with Nsp*V* and inserted into CIC-Nsp*V* that had previously been digested with Nsp*V* to form the CIC chimera. The final chimera, IIC, was made by inserting the *SphI*/*XbaI* fragment from the CIC chimera into Kir2.1 that had similarly been digested with the same enzymes.

All chimeras were sequenced in entirety using the Thermosequenase DNA Sequencing Kit (Amersham). Regions that included PCR products and cut sites were sequenced in both directions.

**c. cRNA Preparation**

For preparation of cRNA, all constructs were linearized with *ScaI*, purified by phenol/chloroform extraction and ethanol precipitation according to standard procedures, and then dissolved in RNase free water at a concentration of 0.5 μg/μl. In vitro transcription was carried out with 1 μg of template DNA using the mESSAGE mACHINE™ Kit (Ambion). The reaction contents included a reaction

buffer that contains salts, buffer, dithiothreitol, among other ingredients. The amount of ribonucleotides added to the reaction varied depending upon the polymerase used, either T3 or Sp6. T3 reactions had 7.5 mM ATP, CTP, and UTP, 1.5 mM GTP, and 6 mM Cap Analog. Sp6 reactions contained 5 mM ATP, CTP, and UTP, and 1mM GTP, and 4 mM Cap Analog. The enzyme mix that was added to each reaction was a buffered 50% glycerol solution containing the appropriate RNA polymerase, placental RNase inhibitor, and "other components which increase the rate and duration of *in vitro* transcription reactions". Reactions progressed at 37°C for 1 hour after which the template was degraded by treatment with RNase-free DNase I for 15 minutes. The RNA was purified by precipitation with 2.5 M LiCl and 25 mM EDTA at -20°C for one half hour. The precipitate was pelleted by centrifugation and subsequently washed with 70% EtOH before resuspending in RNase free water. The lithium chloride precipitation was chosen over phenol/chloroform extraction followed by isopropyl alcohol precipitation because it does not precipitate free ribonucleotides and RNAs smaller than 300 nucleotides. The presence of either of these will lead to exaggerated concentration estimates when determined by UV spectrophotometric methods.

Quantitation of the RNA involved using both the $O.D._{260}$ value and estimation against standard ribosomal RNA of known concentrations when electrophoresed on a 1% agarose gel. RNAs were diluted to the desired 2X concentration and separated into 10 µl aliquots and stored at -80°C. At the time

of injection RNAs were diluted to their final 1X concentration by addition of an equal volume of RNase-free water or a corresponding RNA for co-expression. The amount of RNA injected for Kir2.1 was approximately 0.2 ng. For Kir3.4 and all chimeric channels, the amount injected was 2.0 ng. For all experiments only one batch of RNA was needed. For all co-expression studies, the injections were paired in that individually expressed channels were only compared with co-expression studies from the same batch of oocytes and RNA.

### ii. Oocyte Isolation and Injection

Adult female frogs (*Xenopus laevis*) (Nasco) were anaesthetized in 0.20% MS-222 (Tricaine) and then ovarian lobes were removed by ovarectomy and placed in OR2 solution (82.5 mM NaCl, 2 mM KCl, 1 mM $MgCl_2$, 5 mM Hepes, pH 7.65). Ovarian lobes were manually dissected into small clumps and subjected to treatment with 1 mg/ml collagenase A for 1 hour with gentle shaking to release individual oocytes and remove follicular layer. Oocytes were then rinsed with OR2 solution and treated with 1 mg/ml BSA for 10 minutes with gentle shaking to remove excess collagenase. After 3-4 rinses, individual oocytes were manually separated and placed into modified Barth's solution (MBS) (88 mM NaCl, 1 mM KCl, 0.82 mM $MgSO_4$, 0.33 mM $Ca(NO_3)_2$, 0.41 mM $CaCl_2$, 2.4 mM $NaHCO_3$, 0.5 mM theophylline, 2.5 mM sodium pyruvate, 10 mM Hepes, pH 7.4) containing penicillin (0.0.1 mg/ml), streptomycin (0.01 mg/ml), and gentocin (0.1 mg/ml) to prevent bacterial contamination and stored overnight

in a 17°C incubator. The next day stage V and VI oocytes were selected for injection. The criteria used for selection involved picking oocytes that were spherical in shape, had no associating follicular layer, and had a dark animal pole that was uniform in color and had a sharp border with the vegetal pole. Oocytes were then injected with 46 nl of cRNA solution using a Drummond "Nanoject" Automatic Injector and placed in MBS with antibiotics and stored in a 17°C incubator throughout studies. Unhealthy oocytes were removed and solutions were changed daily.

### iii. Two-Electrode Voltage Clamp

Currents were recorded 1-8 days after injection from oocytes that were bathed in Ringers solution (114 mM NaCl, 2.5 mM KCl, 1.8 mM $CaCl_2$, 1 mM $MgCl_2$, 10 mM Hepes, pH 7.2) containing 150 μM niflumic acid to block $Ca^{++}$-activated chloride currents. Pipettes were filled with 3M KCl and had resistances of 0.5-2.5 MΩ. Data was obtained using a GeneClamp 500 Amplifier (Axon Instruments) and converted to a digital signal using the Digidata 1200 A/D converter which was interfaced to a 486 computer and recorded using pClamp software (Axon Instruments). For recordings in 15 and 40 mM KCl, the NaCl concentrations were adjusted to 101.5 and 76.5 mM, respectively, to maintain osmolarity. All current traces were recorded with and without 1.5 or 2.0 mM BaCl for 15 and 40 mM KCl, respectively, for the purpose of obtaining BaCl-sensitive currents. For I-V relationships, oocytes were clamped at a holding

potential of -70 mV and then pulsed for 200 msec between -120 mV and 20 mV in 10 mV steps with a 10 second interval between pulses. The sampling rate was 20 kHz. For kinetic studies, oocytes were clamped at 10 mV and then pulsed for 50 msec to -100 mV at a sampling rate of 100 kHz. All current traces were filtered at a rate of 2 kHz.

## C. Data Analysis

### i. I-V Relationships

For the presentation of the I-V relationships the average current at the end of each voltage pulse (steady state) between 195 msec and 198 msec for each individual oocyte was imported into Sigmaplot. The mean current levels at each voltage for all oocytes in a particular expression group were plotted against the corresponding voltages. The current traces used were the BaCl-sensitive currents, obtained by subtraction of currents recorded with BaCl from currents recorded without BaCl.

For the determination of extracellular $K^+$ sensitivity, and presence or absence of negative slope, paired t-tests were performed to establish statistical significance. Differences were considered statistically significant with a $p<0.05$. Extracellular $K^+$ sensitivity was measured as the difference between the peak outward currents in 15 and 40 mM extracellular [$K^+$]. Negative slope conductance was measured by comparing the peak outward current level and

the current level at 20 mV. A statistically significant difference was interpreted as being evidence for the presence of a negative slope conductance.

### ii. Absolute Current Levels

Absolute current levels were taken from the mean current levels at -120 mV used for the I-V relationships. Statistical significance between multiple current levels was measured using a One Way ANOVA test with a $p<0.05$ being considered significant. In the event of a significant difference, a Post Hoc test was performed to isolate specific differences. Comparisons between individually expressed channels and the resulting co-expressions only included oocytes from frogs where all three sets were injected and currents measured. In effect, all comparisons are paired so that the effect of batch to batch variability in the quality of oocytes can be minimized.

### iii. Conductance Voltage Relationships

The chord conductance (gK) was calculated for each individual oocyte as follows,

$$gK = I / (V-E_{rev}) \qquad (2)$$

where I represents the steady-state current level at the corresponding voltage, V, and the $E_{rev}$ represents the reversal potential for that individual oocyte. The mean value of gK at each potential for all the studies for a particular expression group was plotted against voltage. For calculation of gKrel the gK values for a

particular oocyte were divided against the gK value at -120 mV for that oocyte. According to equation (2) the value of gK (and gKrel) will approach infinity as the voltage approaches the corresponding reversal potential. As a result of this, the conductance estimate at the voltage that is closest to the reversal potential may have large errors. Therefore, these points were adjusted using a cubic spline function (Sigmaplot) that was measured in 10 mV steps from -120 to 20 mV of the corresponding gKrel-V relationship minus the exaggerated value(s). A cubic spline is a curve that goes through every point and the use of cubic polynomials to describe local segments of the curve will give an estimate of the missing point (s) without effecting the points that do not need to be adjusted (Guardobasso *et al.*, 1988; Motulsky and Ransnas, 1987). The criteria for removing the exaggerated point(s) is as follows: if the reversal potential is within 2.5 mV of a particular voltage, that voltage point is removed. In the case that the reversal potential is greater than 2.5 mV from a particular voltage, then the two adjacent voltages flanking the reversal potential are removed. In essence, the use of the cubic spline adjusts the point or points that do not fit as described by the equation for the calculation of chord conductance. The mean gKrel values for each expression group were plotted against voltage. The resulting curve was then fit to a Boltzmann equation,

$$f(x) = 1/(1 + \exp((x-V_{1/2})/b)) \quad (3)$$

where $V_{1/2}$ is the half maximal voltage, b represents the slope factor, and x is the applied voltage. Comparisons between different gKrel-V relationships were

done between values at particular voltages using the t-test. Significance was demonstrated with a $p<0.05$.

### iv. Time-Dependence of Activation

Time-dependence of activation was measured by fitting the time-dependent component of the currents for test pulses to -100 mV from a holding potential of 10 mV with a monoexponential function using the Simplex method. The time constants or tau were obtained in this fashion. Significance of the differences between multiple expression groups that displayed time-dependence was established using a One Way ANOVA test, followed by a Post Hoc test. Again, a difference was considered statistically significant if $p<0.05$.

# Chapter Three: Study One: Structure-Function Relationships for Kir3.4 and Kir2.1 With Respect to Current Level, $K^+$ Sensitivity, Degree of Inward Rectification, and Time-Dependence of Activation.

## A. Objectives and Hypothesis

The **objective** of Study One was to define the general structural regions of Kir3.4 and Kir2.1 that conferred the properties of current level, extracellular [$K^+$] sensitivity, degree of inward rectification, and time-dependence of activation.

The **hypothesis** was that with respect to current level, the N-terminus would play a more important role for Kir3.4 than it would for Kir2.1 with an equal contribution by the pore region. The reason for this prediction is due to two previous studies. First, in a paper by Lazdunski's group [Fink *et al.*, 1996], chimeras made with the pore and C-terminal regions from Kir3.2, and the N-terminal region from Kir2.3 failed to express. Although not mentioned in the paper, it appears that for the Kir3.0 subfamily the N-terminal region plays a role for current level. Second, Tinker and co-workers presented evidence that for Kir2.1, the M2 and proximal C-terminus was important for homotypic interactions [Tinker *et al.*, 1996], meaning those regions were important for identical subunits interacting to form a homotetramer. With respect to extracellular [$K^+$] sensitivity, the hypothesis is that the pore region should play the dominant role for both Kir3.4 and Kir2.1. The reasoning here is that the pore region contains the only extracellular domains, which is where extracellular $K^+$ would be expected to exert its effect. Finally, the degree of inward rectification and time-dependence of

activation would be defined by both the pore and C-terminal regions for both Kir3.4 and Kir2.1. The reasoning here is that both these properties are directly related to intracellular block of the pore by $Mg^{++}$ and or polyamines. As such, previous studies have already identified some of the important amino acids for $Mg^{++}$ and polyamine binding for Kir2.1, all of which reside in the pore and C-terminal regions. The Kir3.4 clone has not been thoroughly analyzed with respect to these properties, but it was expected that the same regions would be important.

## B. Experimental Design Summary

Kir3.4 and Kir2.1 inward rectifier potassium channels were individually expressed in *Xenopus laevis* oocytes and the resulting currents were characterized with respect to current level, sensitivity to extracellular [$K^+$], degree of inward rectification, and time-dependence of activation. Chimeric channels were constructed from Kir3.4 and Kir2.1 that divided the channels into three general regions. These are the N-terminal region, the pore region, and the C-terminal region. The pore region also includes the membrane spanning domains, M1 and M2, and the proximal C-terminus. The cut sites used were chosen due to restriction sites that were already present in the Kir2.1 clone. The positions of the sites were considered ideal because they separated the two sites shown to be important for inward rectification (D172 and E224 for Kir2.1) and the two regions involved in assembly (M2 and amino acids 230-300 for

Kir2.1). The currents arising from these chimeras were analyzed so that general conclusions could be drawn about which regions conferred the above mentioned properties to each particular wild type channel, either Kir3.4 or Kir2.1.

The size of the currents produced could be influenced by several factors, including number of functional channels on the cell surface, open probability, mean open time, and single channel conductance. The contribution of each of these factors was not measurable in these experiments and therefore were grouped into the general heading of current level. The difference in outward current between 15 and 40 mM extracellular [$K^+$], which either increased or stayed constant, was used as a measure for sensitivity to extracellular [$K^+$]. The degree of rectification was examined both by the presence or absence of negative slope in the outward current, and by the slope factor in the Boltzmann fits for gKrel-V relationships. Finally, the time-dependence of activation was examined by applying current pulses to a highly negative value from a positive holding potential. Currents either displayed an instantaneous jump to a steady-state or showed a time-dependent activation that could be fit with a single exponential function.

## C. Results

### i. Kir3.4 and Kir2.1 Wild Type Currents

#### a. Current Level

Representative current traces from -120 mV to 20 mV in 10 mV steps and a holding potential of -70 mV in 40 mM KCl for Kir3.4, Kir2.1, and water injected oocytes are shown in Figure 3-1a. Mean I-V relationships for Kir3.4, Kir2.1, and water injected oocytes in 40 mM KCl are shown in Figure 3-1b. A bar graph showing the absolute current levels at -120 mV in 40 mM KCl for Kir3.4, Kir2.1, and water injected oocytes is shown in Figure 3-1c. Statistical analysis of the current levels at -120 mV using a One Way ANOVA test showed that there is a significant difference in the current levels ($p<0.001$). A subsequent Post Hoc test was performed to isolate specific differences, and the results showed that all three groups are significantly different from each other ($p<0.05$). It appears from this data that the Kir2.1 channel has a much higher current level than Kir3.4. It should be noted here that this difference becomes more significant when you consider the fact that 10 times as much cRNA was injected for Kir3.4, yet its current level is much lower than Kir2.1.

#### b. $[K^+]_{out}$ Sensitivity

Mean I-V relationships for Kir3.4 and Kir2.1 in both 15 and 40 mM KCl, with an emphasis on the outward current, are shown in Figure 3-2. For Kir3.4 there is no statistically significant increase in the outward current with an

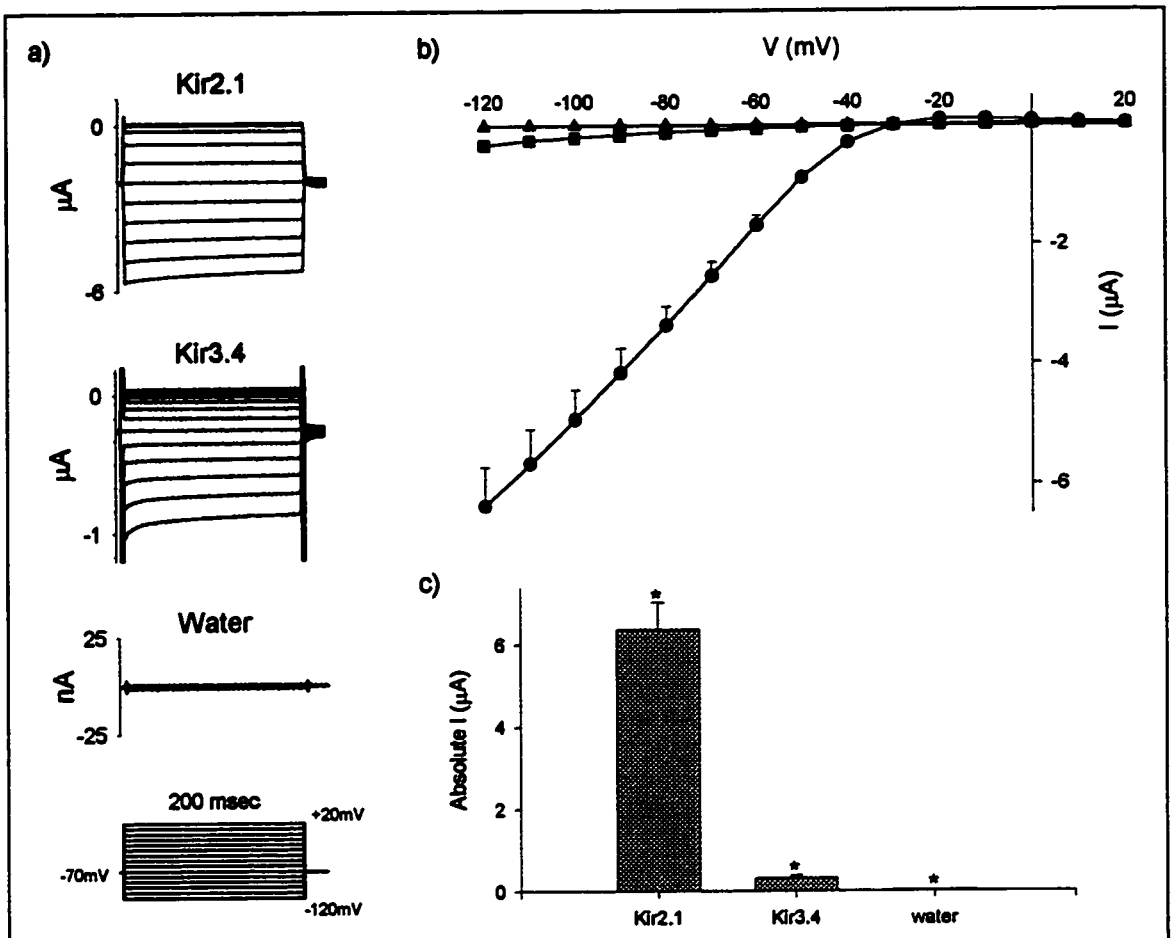


**Figure 3-1. Current Level Comparison for Kir2.1 and Kir3.4.** a) Representative current traces for Kir2.1, Kir3.4, and water injected oocytes in 40 mM KCl. Pulse protocol shown below. b) Mean I-V relationships in 40 mM KCl for Kir2.1 (●, n=15), Kir3.4 (■, n=14), and water (▲, n=5) injected oocytes. c) Absolute current levels at -120 mV for Kir2.1, Kir3.4, and water injected oocytes. Asterisks indicate statistical significance between all 3 groups ($p<0.05$).

increase in extracellular $K^+$ ($p>0.05$). However, Kir2.1 does show a statistically significant increase in the outward current when the extracellular $K^+$ level is increased from 15 mM KCl to 40 mM KCl ($p<0.01$).

### c. Degree of Rectification

Also important in Figure 3-2 is the presence or absence of negative slope in the outward current. For Kir2.1, a paired t-test showed the current level at

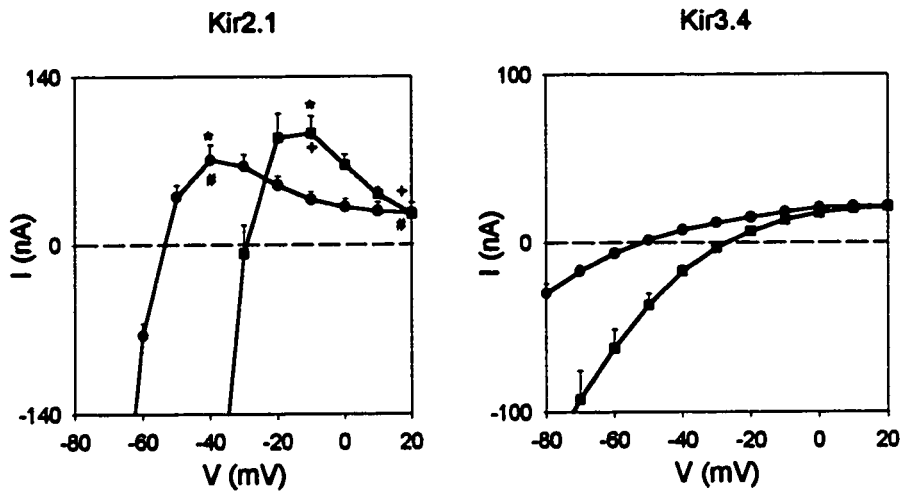


**Figure 3-2. Outward Current Comparison for Kir2.1 and Kir3.4.** Mean I-V relationships for Kir2.1 and Kir3.4 in 15 (■) and 40 (●) mM KCl. Kir2.1 currents show a statistically significant increase in outward current with 40 mM extracellular [$K^+$], and a prominent region of negative slope conductance that is absent in the Kir3.4 currents. Statistically significant differences are indicated by symbols shown at the corresponding current levels ($p<0.01$).

either -40 mV or -10 mV for the 15 and 40 mM KCl traces, respectively, was statistically greater than the current level at +20 mV, indicating the presence of a negative slope conductance ($p<0.05$). This is in contrast to Kir3.4 where at positive potentials the current continues to increase with no evidence of a negative slope conductance. These data indicate that the degree of rectification is stronger in Kir2.1 than it is in Kir3.4.

The mean conductance (gK) versus voltage relationships for Kir3.4 and Kir2.1 are shown in Figure 3-3a. In addition, the gK at each voltage for each individual oocyte was normalized to the gK value at -120 mV. The resulting gKrel-V relationship is shown in Figure 3-3b. The qualitative difference between

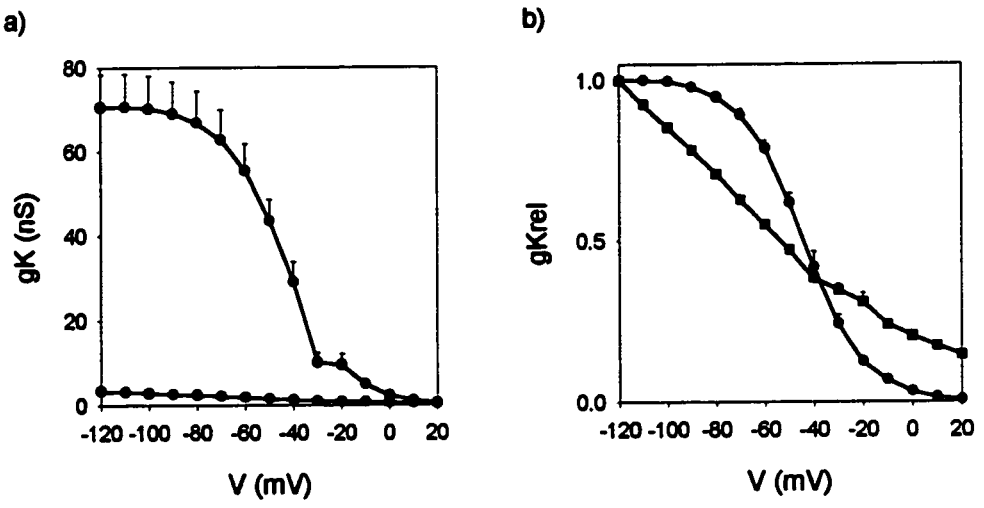


**Figure 3-3. Conductance-Voltage Relationships for Kir2.1 and Kir3.4.** a) Mean gK-V relationships for Kir2.1 (●) and Kir3.4 (■). b) Normalized gKrel-V relationships for Kir2.1 and Kir3.4. Kir2.1 shows a sigmoidal relationship where the conductance saturates around -100 mV, while the conductance for Kir3.4 does not saturate in this range.

the channels becomes obvious. The Kir2.1 gKrel relationship follows a sigmoidal curve that fits a single Boltzmann, shown in Figure 3-4a, with a $V_{1/2}$ of -44.3 mV and a slope factor of 12.2. The Kir3.4 current however does not show a sigmoidal curve and cannot be used to esimate the a parameters in the Boltzmann equation. The difficulty in fitting the Kir3.4 gKrel-V relationship to a Boltzmann equation may be due to the lack of saturation in the conductance levels. If this is the case, then the use of the conductance level at -120 mV as the gmax value, for the normalization of conductance, is incorrect. However, attempts to fit the g-V relationship for Kir3.4 using gmax as a free parameter

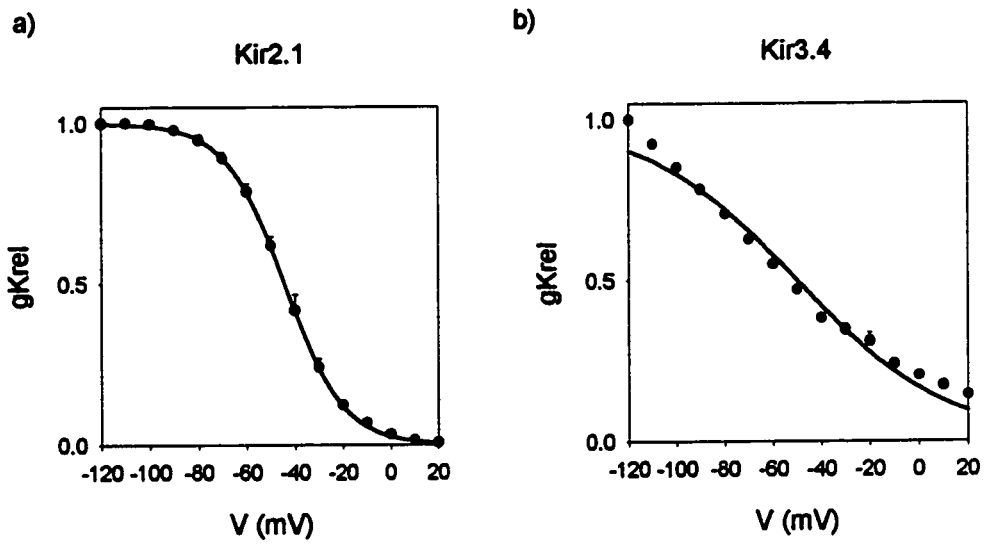


**Figure 3-4. Boltzmann Fits to gKrel-V Relationships for Kir2.1 and Kir3.4.** a) Kir2.1 Boltzmann fit with a v½ of -44.4 mV and a slope factor of 12.2. Visual inspection shows close approximation of the fit to the data points. b) Attempted Boltzmann fit to Kir3.4 gKrel-V relationship. Curve visually does not fit as the conductance does not saturate.

were unsuccessful. Regardless, the important point is that there is a striking qualitative and quantitative difference between Kir2.1 and Kir3.4 with respect to their conductance voltage relationships.

### d. Time-Dependence of Activation

Representative current traces for 50 msec pulses to -100mV from a holding potential of +10 mV in 15 mM KCl are shown for both Kir3.4 and Kir2.1 in Figure 3-5. Qualitatively there is an obvious difference between the two in that the Kir3.4 current trace shows only an instantaneous step in current with no evidence of a time-dependent increase in amplitude. The Kir2.1 trace, however, shows a significant time-dependent increase that can be fit with a single

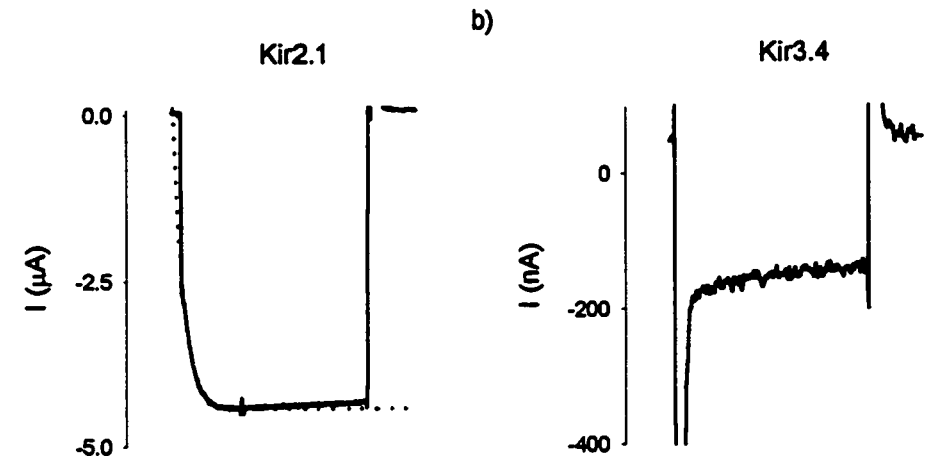


**Figure 3-5. Time-Dependent Activation for Kir2.1 and Kir3.4.** Representative current traces for 50 msec current pulses to -100 mV from a holding potential of +10 mV for both a) Kir2.1, and b) Kir3.4. The Kir2.1 trace shows an obvious time-dependent component that can be fit with a single exponential function (shown as dotted line) with a tau of 2.19 msec. The Kir3.4 trace shows no time-dependence and could not be fit with a single exponential function.

exponential function. The tau is 2.19 +/- 0.18 msec. The time-dependence of activation for Kir2.1 likely represents unblock of the pore by internal polyamines. The lack of time-dependence for activation for Kir3.4 suggests a different mechanism of activation when compared to Kir2.1. It should be noted that the smaller current size for Kir3.4 may have made it impossible to resolve any time-dependent component, due to a possible masking effect of the capacitive transient. However, even the largest of the Kir3.4 currents (shown in Figure 3-5) showed no evidence of a time-dependent component.

## ii. Kir3.4/Kir2.1 Chimera Currents

### a. Current Level

Only three of the six chimeras produced any significant current when injected into *Xenopus* oocytes: the ICI, CCI, and CII chimeras. Representative current traces from -120 mV to +20 mV in 10 mV steps from a holding potential of -70 mV in 40 mM for the three current producing chimeras are shown in Figure 3-6a. Mean I-V relationships for ICI (n=7), CCI (n=8), and CII (n=7) along with Kir2.1 and Kir3.4 for comparison are shown in Figure 3-6b. The absolute current level at -120 mV for all chimeras and Kir3.4 and Kir2.1 are shown in Figure 3-6c. Statistical analysis using a One Way ANOVA and a Post Hoc test showed there is a statistically significant difference between the current levels ($p<0.001$). Specifically, Kir2.1 was different from all other currents, Kir3.4 was different from all other currents except CCI, and finally, ICI was different from all others except CII ($p<0.05$). The two chimeras ICI and CII are larger than Kir2.1 which is understandable considering ten times as much cRNA was injected for the mutants. Finally, all of the non-functional chimeras showed a current level that was not significantly different than water injected oocytes ($p>0.05$).

### b. $[K^+]_{out}$ Sensitivity

Figure 3-7 shows the mean I-V relationships for the three current producing chimeras, along with Kir3.4 and Kir2.1 for comparison, in 15 and 40 mM KCl, with an emphasis on the outward current. The chimeras ICI and CII are

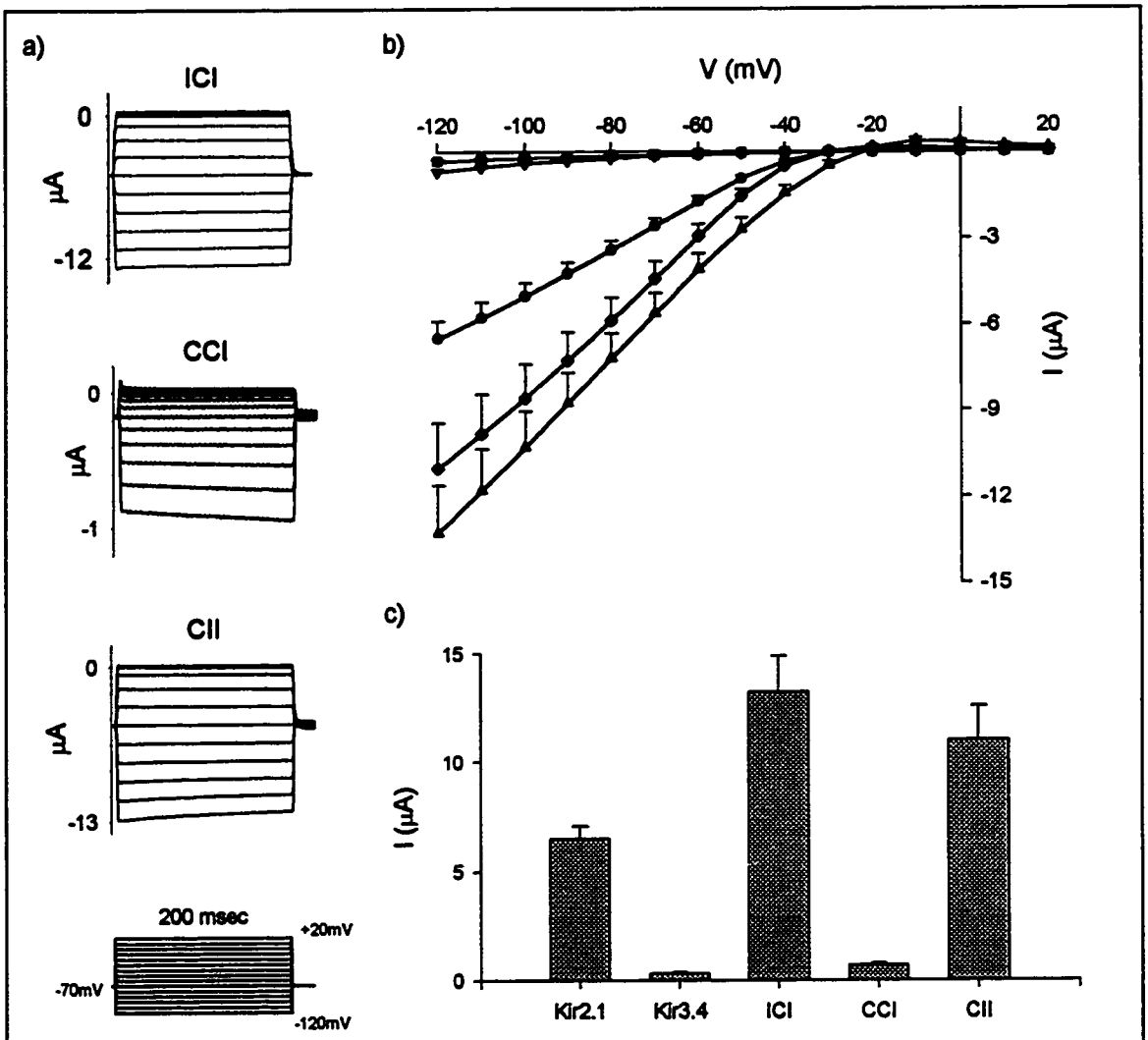


**Figure 3-6. Current Level Comparison for ICl, CCl, and CII.** a) Representative current traces for ICl, CCl, and CII injected oocytes in 40 mM KCl. Pulse protocol shown below. b) Mean current-voltage relationships in 40 mM KCl for ICl (▲, n =7), CCl (▼, n=8), CII (◆, n=7), and Kir2.1 (●) and Kir3.4 (■) for comparison. Error bars show + standard error of the mean (SEM). c) Absolute current levels at -120 mV for ICl, CCl, and CII, with Kir2.1 and Kir3.4 shown for comparison.

similar to Kir2.1 in that there was a statistically significant increase in the outward current when the extracellular [$K^+$] level was raised from 15 to 40 mM KCl ($p<0.05$). The third chimera, CCl, is more similar to Kir3.4 in that there is no

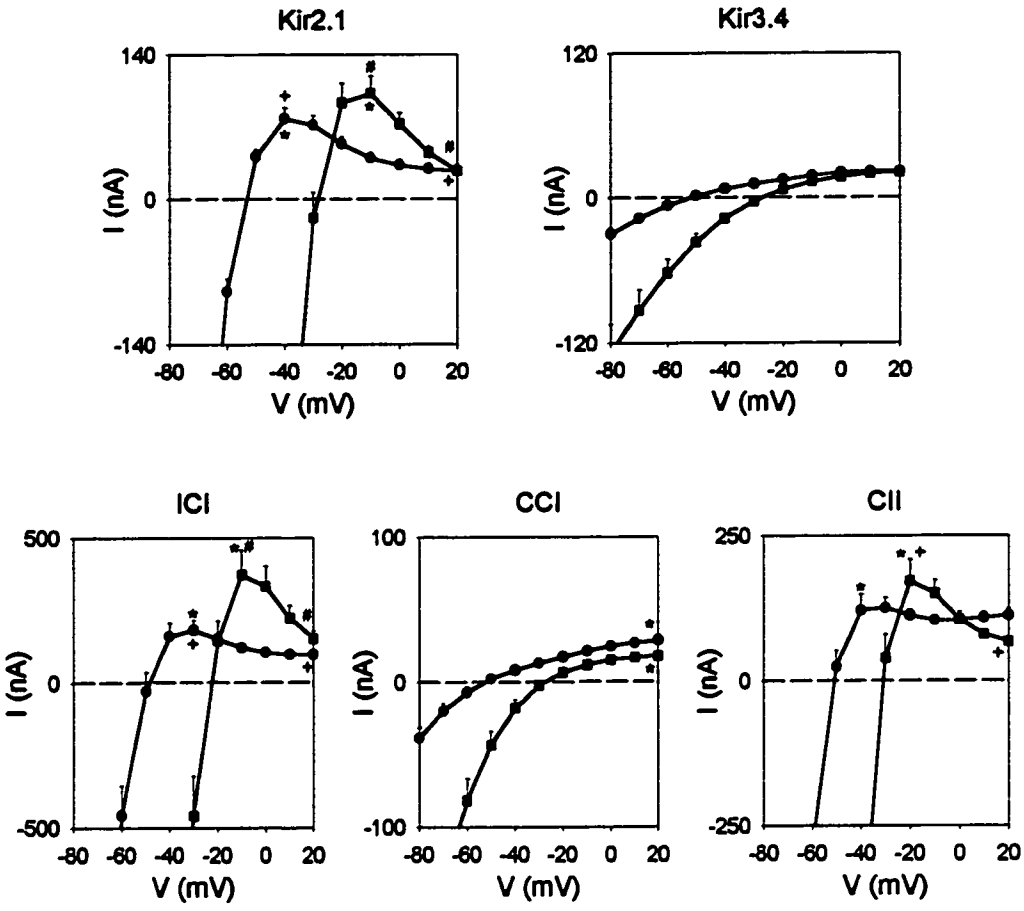


**Figure 3-7 Outward Current Comparisons for ICl, CCl, and CIl.** Mean I-V relationships for ICl, CCl, and ICl with Kir2.1 and Kir3.4 shown for comparison. The extracellular [$K^+$] were 15 (●) and 40 (■) mM. Symbols indicate statistical significance between corresponding current levels ($p<0.05$).

increase in the outward current. Actually, the outward current actually decreases where the difference is statistically significant ($p<0.05$).

**c. Degree of Rectification**

Also shown in Figure 3-7, is the presence or absence of a region of negative slope conductance. As with sensitivity to extracellular [$K^+$], chimeras ICI and CII are more similar to Kir2.1 than Kir3.4. For both of these chimeras there is a statistically significant difference between the current level at -40 mV or -10 mV for 15 and 40 mM KCl, respectively, and the current level at 20 mV ($p<0.05$). This is in contrast to the CCI chimera which, like sensitivity to extracellular $K^+$, is much more similar to Kir3.4 than it is to Kir2.1. The current level continues to increase as membrane potential is made more positive with no evidence of a negative slope conductance.

Shown in Figure 3-8a is the gK versus voltage relationships for chimeras ICI, CCI, and CII along with Kir3.4 and Kir 2.1 for comparison. Figure 3-8b shows the gKrel-V relationships for the same currents. Again it can be seen that the ICI and CII chimeras were more similar to Kir2.1 in that they also have displayed a sigmoidal shape in their respective gKrel-V relationships. Both curves fit a single Boltzmann equation shown in Figure 3-9. However, the ICI chimera has a $V_{½}$ of -32.6mV and a slope factor of 17.3, which is significantly different from that of Kir2.1 (-44.4 mV and 12.2, respectively). This suggests that although similar to Kir2.1, the ICI chimera is not as strong an inward rectifier. The CII chimera has a $V_{½}$ of -42.8mV and a slope factor of 14.4 which are not significantly different from that of Kir2.1. The remaining chimera CCI had a gKrel-V relationship that does not fit a Boltzmann equation (Figure 3-9) and is

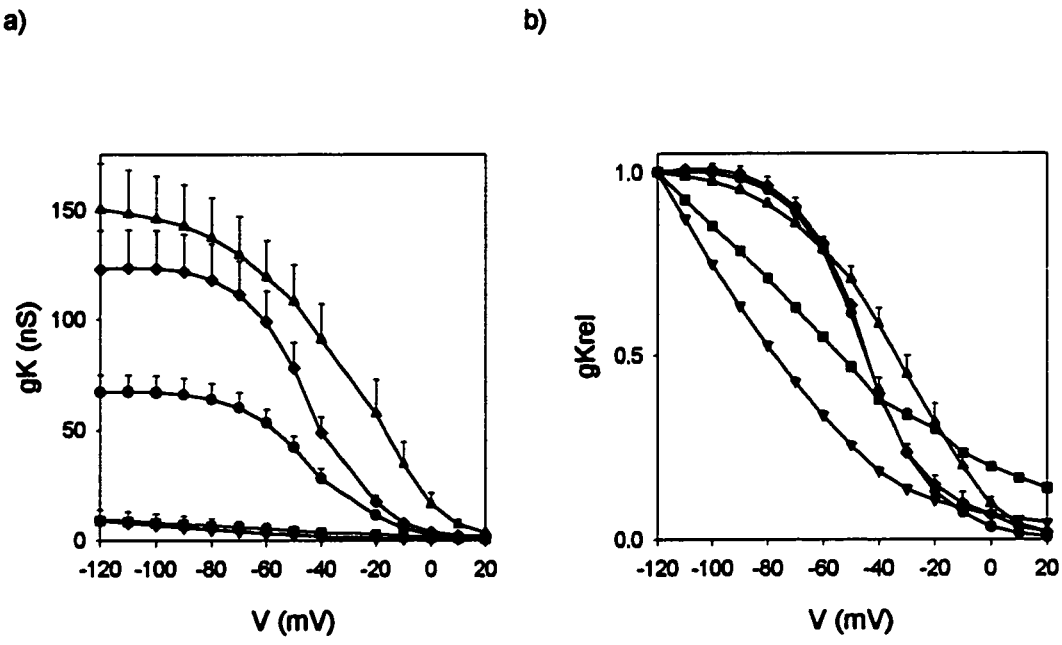


**Figure 3-8. Conductance-Voltage Relationships for ICI, CCI, and CII.** a) gK-V relationships and b) gKrel-V relationships showing mean values for Kir2.1(●), Kir3.4(■), ICI(▲), CCI(▼), and CII(◆). Error bars show + standard error of the mean(+SEM).

similar to Kir3.4 in that the conductance does not saturate. This indicates that the CCI chimera has rectification properties that are more similar to Kir3.4.

### d. Time-Dependence of Activation

Figure 3-10 shows representative currents elicited by pulses to -100mV for 50 msec from a holding potential of +10 mV for ICI, CCI, and CII. Again we see the same pattern in that ICI and CII are similar to Kir2.1 and CCI is similar to Kir3.4. ICI and CII show a time-dependence of activation, similar to that of Kir2.1, that could be fit with a single exponential function, giving values of 1.51 ± 0.11 msec and 2.41 ± 0.22 msec, respectively, for the time constant tau. In

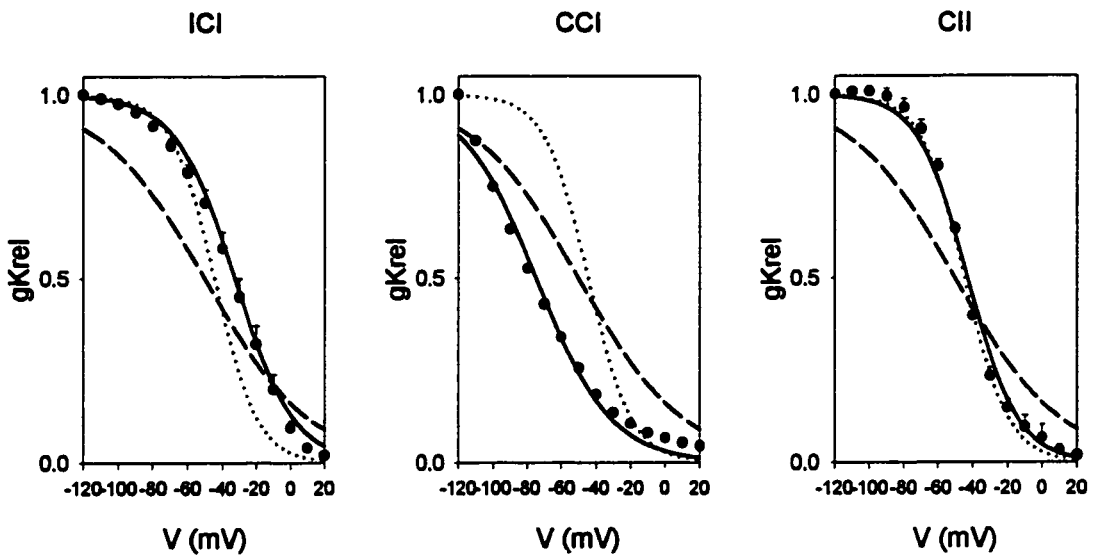


**Figure 3-9. Boltzmann fits for ICl, CCl, and CIl.** Each gKrel-V relationship for ICl, CCl, and CIl shows data points with corresponding fit (solid line). The fits for Kir2.1 (dashed line) and Kir3.4 (dotted line) are also shown for comparison.

contrast, CCl shows only instantaneous current similar to the Kir3.4 wild type current. Again, it should be noted that the small current size for CCl, relative to the capacitive transient, may have made it difficult to resolve any time-dependent component. However, the largest CCl currents did not show any evidence for a time-dependent component.

## D. Discussion

A summary of the results for Study One can be found in Table 3-1. A review of the results for the wild type Kir3.4 and Kir2.1 channels reveals that for each property studied there is a contrast: the Kir3.4 clone shows a relatively low

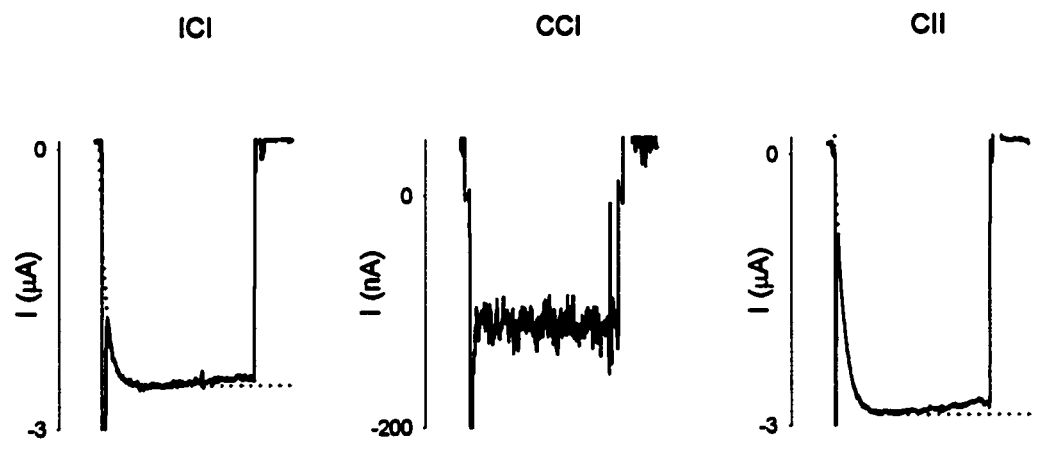


**Figure 3-10. Time-Dependence of Activation for ICl, CCl, and CIl.** Representative current traces from 50 msec pulses to -100 mV from a holding potential of +10 mV in 15 mM KCl for ICl, CCl, and CIl. Both ICl and CIl fit a single exponential function which is shown for each (dashed line). The CCl trace does not fit a single exponential function.

current level, no increase in outward current with a corresponding increase in extracellular [$K^+$], no region of negative slope conductance, no saturation of conductance at -120 mV, and a lack of time-dependence for activation. With Kir2.1 there is a higher current level, an increase in outward current at higher extracellular [$K^+$], a prominent region of negative slope conductance, a saturating conductance-voltage relationship that fits a Boltzmann model, and definite time-dependence of activation when pulsing from a positive holding potential. The results involving the chimeric channels parallel those for the wild type, in that the channels that show a high current level, ICl and CIl, also show extracellular [$K^+$] sensitivity, negative slope conductance, a saturating conductance-voltage relationship, and a time-dependent activation, which is in

**Table 3-1. Summary of Results for Study One.** An entry of n/a means not applicable as no current was present for evaluation. gKrel-V values indicate the $V_{1/2}$ and slope factor for single Boltzmann fits to the corresponding relationship.

| Channel | Current Level | Sensitivity to $[K]_{out}$ | Negative Slope | gKrel-V | Time Dependence |
|---|---|---|---|---|---|
| Wild Type | | | | | |
| Kir3.4 | low | no change | no | no fit | no |
| Kir2.1 | high | increase | yes | -44.4mV, 12.2 | yes |
| Chimeras | | | | | |
| ICI | high | no change | yes | -32.6mV, 17.3 | yes |
| ICC | none | n/a | n/a | n/a | n/a |
| CCI | low | decrease | no | no fit | no |
| CIC | none | n/a | n/a | n/a | n/a |
| CII | high | increase | yes | -42.8mV, 14.4 | yes |
| IIC | none | n/a | n/a | n/a | n/a |

contrast to the chimera CCI, which had a low current level that did not exhibit any of these properties.

As seen in Figure 3-1 there is an obvious difference in the current levels between Kir2.1 and Kir3.4, with the average Kir2.1 current being approximately seven times larger at -120 mV than the Kir3.4 current at the same voltage. This difference becomes more significant when you consider the fact that Kir2.1 had ten times less RNA injected than Kir3.4. As previously mentioned, the level of

current may be influenced by several factors that include number of functional channels of the cell surface, open probability, mean open time, and single channel conductance. None of these parameters were measured in the present study, however, previous studies from other investigators have measured some of these properties for both Kir2.1 and Kir3.4. The most striking differences between Kir2.1 and Kir3.4 are seen when comparing their respective single channel properties. Specifically, Kir2.1 shows a single channel conductance of 21 pS and a relatively long open time and open probability [Kubo *et al.*, 1993], which is in sharp contrast to Kir3.4 which shows brief and poorly resolved channel openings that makes an accurate calculation of single channel conductance and open-time kinetics difficult [Chan *et al.*, 1996]. With respect to measuring surface expression, studies on Kir2.1 are not available, however, Kir3.4 has been analyzed in this regard. Apparently, the low current level cannot be attributed to low surface expression as it has been shown by Clapham's laboratory that Kir3.4 localizes to the plasma membrane when transfected in COS cells [Kennedy *et al.*, 1996]. Also, studies on another member of the Kir3.0 subfamily, Kir3.2, have shown using immunofluorescence that high levels of surface expression can be obtained in *Xenopus* oocytes [Stevens *et al.*, 1997]. When considering these studies, it seems reasonable to say that the large difference in current level between Kir2.1 and Kir3.4 is most likely due to their differences in gating characteristics, and not due to a large difference in expression of functional channels on the cell surface.

Another striking difference between Kir2.1 and Kir3.4 can be seen in Figure 3-2, which focuses on the outward currents produced by these channels. It is obvious from the figure that the Kir2.1 channel shows an increase in outward current when the extracellular $K^+$ concentration is raised from 15 to 40 mM while the Kir3.4 channel shows no change. Also, Kir2.1 shows a statistically significant region of negative slope conductance while Kir3.4 does not. Two questions come to mind when considering at these results. First, what are the properties of sensitivity to extracellular [$K^+$] and negative slope conductance telling us about the particular channel? Second, why is there is such a difference between Kir2.1 and Kir3.4? Insight into these questions may be obtained by considering the mechanism of inward rectification.

The mechanism of inward rectification involves intracellular block of the pore region by $Mg^{++}$ and/or polyamines [Matsuda, 1991; Matsuda *et al.*, 1987; Vandenberg, 1987; Lopatin *et al.*, 1994; Lopatin and Nichols, 1995]. At potentials negative to $E_K$, a blocking particle in the pore region can be displaced by electrostatic repulsion from incoming $K^+$ ions, resulting in inward current. At potentials positive to $E_K$, $K^+$ ions are prevented from exiting the cell through the pore because of the blocking effect of $Mg^{++}$ or polyamines. The size of the outward current at any particular voltage positive to $E_K$ will depend upon how many channels are blocked. Therefore, as the potential becomes more positive, more channels become blocked resulting in less outward current. It should be noted that this is an oversimplified view of the mechanism of inward rectification.

There are numerous factors involved in determining the degree of rectification: the voltage-dependent binding of the blocker(s), the electrochemical nature of the blocker(s), the number and location of the binding site(s), and the strength of the interaction between the blocker(s) and the binding site [Hille, 1992; Hille and Schwarz, 1978; Lopatin and Nichols, 1996].

The difference in results for presence or absence of negative slope between Kir2.1 and Kir3.4 suggests a variation in the blocking relationships between the channels and intracellular blockers. The negative slope conductance seen with Kir2.1 is the result of a strong interaction between the intracellular blockers and the pore region at positive potentials, to the point that outward current is almost completely abolished. For Kir3.4, the interaction between the blockers and the pore is not as strong, so at the more positive potentials outward current can still increase to a limited extent so that no region of negative slope is seen. These results are not surprising if the important sites for rectification, as mentioned in the introduction and shown in Figure 2-1, are considered. Kir2.1 has a negative charge in both important sites, D172 and E224, while Kir3.4 has a neutral and negative charge for the equivalent sites, N179 and E231, respectively. The presence of two negative sites for Kir2.1 compared to only one for Kir3.4 would suggest that Kir2.1 may provide a stronger binding site for $Mg^{++}$ and polyamines and would, therefore, show stronger inward rectification.

Binding of $Mg^{++}$ and polyamines at the internal side of the pore region produces inward rectification, but at higher extracellular concentrations $K^+$ ions can bind at an external binding site that is relatively close to the pore and the internal binding site for the blocking cation. At potentials just positive to $E_K$, the electrostatic repulsion between the bound $K^+$ and blocking cation are sufficient to knock the blocker off the binding site on the channel. However, as the potential moves more positive, the electrochemical gradient for the blocker becomes stronger as it begins to repel $K^+$ and reoccupy its own binding site. In short, at low extracellular $[K^+]$ the onset of rectification begins around $E_K$, while at higher extracellular $[K^+]$ the onset of rectification is shifted to potentials positive of $E_K$ (Kubo, 1996). The end result is that as the extracellular $K^+$ concentration is increased, more outward current is seen because of this shift in rectification. The results for $[K^+]$ sensitivity of Kir2.1 indicate that the channel is affected by binding of $K^+$ ions to an external binding site, shifting rectification along the voltage axis and resulting in more outward current at elevated extracellular $[K^+]$. For Kir3.4, the absence of any increase in outward current suggests that there is no binding site for extracellular $K^+$ ions present, or at least not a site that can affect rectification to the point where an increase in outward current is seen when $[K^+]$ is increased.

Another measure of rectification can be seen in Figure 3-3 with the conductance-voltage relationships for Kir2.1 and Kir3.4. The large difference in conductance between the two channels made it difficult to compare their

respective gK-V relationships. Therefore, the conductance levels at each voltage were normalized to the conductance at -120 mV to produce a gKrel-V relationship (Figure 3-3b). Again, an obvious difference between Kir2.1 and Kir3.4 is apparent, with Kir2.1 showing a sigmoidal relationship that can be fit with a single Boltzmann function (Figure 3-4), but this is not the case for Kir3.4. What does this say about each channel? The Boltzmann model for the gKrel-V relationship has been used by others to imply that inward rectification is a result of a first-order steady-state binding reaction between channel subunits and internal polyamines [Lopatin *et al.*, 1994; Glowatzki *et al.*, 1995]. The model itself describes the voltage-dependence for two different energy states for the channel. The $V_{½}$ is the voltage where half of the channels are blocked by polyamines and the slope factor is a measure of the voltage-sensitivity of the interaction. The voltage-sensitivity of the interaction depends upon the charge of the blocker and the electrical distance, or fraction of the total electrical potential drop, of the binding site [Hille, 1992; Lopatin *et al.*, 1994]. A smaller slope factor means you have a steeper curve that suggests stronger rectification when compared to a shallower curve with a higher slope factor. This is an oversimplified view, but the fact that the Kir2.1 gKrel-V relationship fits this model and Kir3.4 doesn't suggests, either a different mechanism for rectification, or a different blocking particle and or binding site. However, the curve in Figure 3-3b for Kir3.4 shows that the conductance level does not saturate, but continues to increase even as the potential gets more negative. Therefore, it is

conceivable that the gKrel-V relationship for Kir3.4 would fit a Boltzmann function if a larger range of voltages had been analyzed. In any event, there is a difference, between Kir2.1 and Kir3.4, that can only be explained by variations in pore block and or a fundamental difference in their respective mechanisms for rectification.

The final comparison between Kir2.1 and Kir3.4 is shown in Figure 3-5 where the Kir2.1 current is shown to have a time-dependent component when the voltage is pulsed to a negative value from a positive holding potential. Kir3.4 shows only an instantaneous component. These contrasting results can also be explained by the differences in rectification. Unblock of the channel by polyamines at highly negative potentials is thought to produce the time-dependence of activation (Ishihara and Hiraoka, 1994). The time-dependence of activation does not include unblock of $Mg^{++}$ from the pore as this has been shown to be virtually instantaneous (Ishihara and Hiraoka, 1994). The Kir2.1 channel shows an obvious time-dependent activation that is fit with a single exponential function which describes the unblocking rate of polyamines from the channel. The Kir3.4 channel does not show any time-dependence of activation. This may indicate that this channel is either not blocked by polyamines or that unblock of polyamines is instantaneous due to a weak interaction. However, it should be re-emphasized that any time-dependent component for Kir3.4 may have been masked by a relatively larger capacitive transient, although analysis

of the largest Kir3.4 currents did not indicate the presence of any time-dependent component.

To summarize so far the Kir3.4 channel produces a relatively low level of current that does not display the properties, seen with Kir2.1, such as extracellular [$K^+$] sensitivity, negative slope conductance, saturating conductance-voltage relationship, and a time-dependence for activation. Anaylsis of the chimeric channels revealed a similarity in that the absence of these properties coincides with a relatively small current level. With this in mind, the question becomes, what structural regions of Kir3.4 are required to imitate the lower current level that lacks any of the properties associated with Kir2.1?

Of the three chimeric channels to show a current, only the CCI chimera displayed properties similar to Kir3.4: a low current level with no sensitivity to extracellular [$K^+$], no negative slope conductance, no saturation of conductance at -120 mV, and no time-dependent activation (Figures 3-6 through 3-9). This suggests that the important regions for these characteristics of Kir3.4 are present in the N-terminal and pore regions since the chimera derived both of these regions from Kir3.4, while the C-terminal region was donated by Kir2.1. Moreover, the other two expressing chimeras, ICI and CII, did not display Kir3.4-like properties, which suggests that both the N-terminal and pore regions of Kir3.4 are necessary in order to imitate the Kir3.4 current.

A look at the two chimeras that express at a high current level will reveal that they parallel the Kir2.1 current in that they display the properties of

sensitivity to extracellular [$K^+$], negative slope conductance, saturation of conductance at more negative potentials, and time-dependent activation (Figures 3-6 through 3-9). The only significant difference between Kir2.1 and any of the chimeras is the values for the $V_{½}$ and slope factor for the Boltzmann fits between Kir2.1 and ICI. The gKrel-V relationship for ICI is shallower than Kir2.1 which can be confirmed by the different slope factors of 12.6 and 19, respectively. This is not surprising considering the sites for rectification already discussed. ICI has N179 from Kir3.4 and E224 from Kir2.1 (Figure 2-1). This difference in one negative charge can explain why ICI showed a shallower gKrel-V relationship, since, as already mentioned, the slope factor depends upon the electrical position of the binding site.

So for the chimeras that express a current, the common theme is that the C-terminal region of Kir2.1 is present in all of them. The size of the current is then dependent upon the corresponding N terminal and pore regions. In the event that either is from Kir2.1, the resulting current is large and displays sensitivity to extracellular [$K^+$], negative slope conductance, a saturating conductance voltage relationship that fits a Boltzmann model, and time-dependent activation. When both the N-terminal and pores are from Kir3.4 the resulting current is relatively small without these properties. For the chimeric channels that failed to produce a current there is also a common theme. All three of these channels contained the C-terminal region for Kir3.4. It appears that the C-terminal region from Kir3.4 is only compatible with the N-terminal and

pore regions from Kir3.4. This is opposite for Kir2.1 whose C-terminal region appears to be compatible with any combination of N-terminal and pore regions, whether they are from Kir2.1 or Kir3.4. Any statements regarding these observations would be pure speculation as there is no way of knowing whether these nonfunctional channels failed to assemble properly or produced channels with either a permanent inactivation or a non-conducting pore.

To summarize, the currents analyzed here fall into one of two groups that differ by the size of the current level, either large or small. The large currents all display properties associated with the mechanism of inward rectification. That is, they all show extracellular [$K^+$] sensitivity, negative slope conductance, saturating conductance-voltage relationships, and time-dependent activation. The smaller currents do not display any of these properties. However, this is not to say that the rectification properties are not seen due to small current size because, theoretically, all of the properties measured should be evident regardless of the current level. Indeed, in unrelated studies, small amplitude currents were obtained for Kir2.1, comparable to Kir3.4 currents, that displayed the properties of extracellular [$K^+$] sensitivity and negative slope conductance. A more likely scenario is one where the smaller current size is due to a fundamental difference in the conductance and gating properties of Kir3.4 when compared to Kir2.1.

Hille and Schwarz originally modelled potassium channels, including inward rectifiers, as containing a multi-ion single file pore, where the channel

could contain more than one ion at a time, each of which could hop in single file into vacant sites with rate constants that depend on energy barrier heights, membrane potential, and interionic repulsion [Hille and Schwarz, 1978]. These investigators used this model to back up Armstrong's hypothesis that inward rectification could be understood in terms of block by an internal cation [Armstrong, 1969]. As already mentioned, the internal cations are $Mg^{++}$ and polyamines. As such, the opening and closing, or gating, of inward rectifiers, as described by this model, is determined by these soluble gating particles. A recent study on the Kir2.1 clone is in general agreement with this model [Lopatin and Nichols, 1996], however, Kir3.4 has not been analyzed in this regard. The data in this study suggest that Kir3.4 maybe subject to an entirely different gating mechanism.

The gKrel-V relationship for Kir2.1 is, in essence, a representation of the open probability of the channel, where at negative potentials all of the channels are open, or not blocked by a soluble gating particle, and at positive potentials the majority of channels are closed, or blocked by a soluble gating particle. For Kir3.4 and CCl, the lack of saturation of conductance at more negative potentials suggests that not all of the channels are open. Are these closed channels blocked by a soluble gating particle, or are they subjected to a different gating mechanism? If they are blocked by a soluble gating particle, similar to Kir2.1, then you would expect to see, considering a relativley large degree of homology with Kir2.1, the properties of rectification being demonstrated, as expected from

the multi-ion single file pore model proposed by Hille and Schwarz. If not pore block, what other gating mechanisms are possible?

There have been numerous theories proposed describing the nature of gates [Hille, 1992], including block by either a soluble or tethered blocker. Indeed, Dascal and co-workers suggested that block of Kir3.1 channels was achieved by C-terminal tail block [Dascal *et al.*, 1995]. However, careful review of the data in the paper presented by Dascals group will reveal that their results could also be explained by a competition for available Gβγ subunits. In any event, the mechanism that is responsible for the level of inactivation in the absence of G-protein stimulation, seen with members of the Kir3.0 subfamily, has not been firmly established. One possible mechanism that has not been proposed in the literature is that the channels are in a non-conducting configuration that can be altered when Gβγ binds the channel, thus activating it. The channel is non-conducting due to a destabilization effect on the selectivity filter. Random and short-lived transitions to the conducting state allow for the brief current steps, seen in other studies that have attempted single channel analysis, and are short enough that the properties of pore-block are not evident. Transitions to the conducting state are voltage-dependent in that with increasing hyperpolarization, more and more channels make the brief transition so that more current is seen. Evidence supporting this model is provided by two previous studies that together suggest that destabilization of the selectivity filter results in a channel that has conductance properties that are simliar to Kir3.4.

First, a study by the Jan laboratory identified two amino acids, E138 and R148, that together form a salt bridge that is necessary for stabilization of the selectivity filter [Yang *et al.*, 1997]. Any alteration of these sites dramatically alters permeation. Second, in another study by Kubo, aimed at identifying molecular determinants for sensitivity to extracellular [$K^+$], involved mutating R148 to a tyrosine [Kubo, 1996]. The R148Y mutant produced currents that were almost identical to individually expressed Kir3.4 subunits: lower current level, no sensitivity to extracellular [$K^+$], and a non-saturating conductance level at -200 mV.

In the event that the model presented is accurate, then you would expect that with full activation of all of the Kir3.4 channels the resulting conductance-voltage relationship would show saturation. A previous study by Iizuka and co-workers, showed that when Kir3.4 was co-expressed with Gβγ subunits the resulting current, although 150% larger than individually expressed Kir3.4 subunits, did not achieve saturation [Iizuka *et al.*, 1996]. However, no indication of how much cRNA was injected was stated, so it is not known if the amount of Gβγ subunits injected was enough to fully activate all of the channels. This model becomes even more complex when you consider the fact that Kir3.4 co-assembles with Kir3.1 to form the physiological channel $I_{KACh}$ [Krapivinsky *et al.*, 1995b]. In the absence of Gβγ stimulation, Kir3.1 and Kir3.4 complexes produce currents that saturate, while the presence of Gβγ reduces saturation [Iizuka *et al.*, 1996]. In any event, future studies revolving around this model should

attempt to determine the effect of Gβγ on Kir3.4 currents. That is, does binding of Gβγ to Kir3.4 change the conductance and gating properties so that it is similar to Kir2.1, or does it just affect open time kinetics.

The model presented above is pure speculation, and therefore, further studies would be required to support or disprove the model. In any case, the data obtained in this study show a large difference between individually expressed Kir2.1 and Kir3.4 subunits. The chimera data suggest that the N-terminal and pore regions of Kir3.4 seem critical for displaying the low current level that shows no sensitivity to extracellular [K+], no negative slope conductance, no saturation of conductance at -120 mV, and no time-dependence of activation. Previous studies suggest that the large difference in current levels are not due to insufficient cell surface expression of Kir3.4 relative to Kir2.1, but rather, fundamental differences in gating and conductance properties. Future studies should therefore be directed at analyzing the molecular determinants of Kir3.4 that are responsible for the difference in these properties.

# Chapter Four: Study Two: Structural Determinants for Interaction Between Kir2.1 and Either Kir3.4 or Kir2.1/Kir3.4 Chimeric Channels.

## A. Objectives and Hypothesis

The **objective** of Study Two was to determine whether Kir3.4 and Kir2.1 can interact when co-expressed in *Xenopus* oocytes and generally define the structural regions that are necessary for interaction, or lack thereof.

The **hypothesis** was that if there is any interaction between the pore-forming subunits, it would be a dominant-negative effect of Kir3.4 on Kir2.1. A dominant-negative subunit would have the ability to interact with another subunit and abolish any current in a dominant fashion. This prediction is based on previous studies. Adelman's group [Tucker *et al.*, 1996] showed that Kir3.4 had a dominant-negative effect on Kir4.1, and Kunkel and Peralta [Kunkel and Peralta, 1995] showed the same effect of Kir3.4 on rbIrk2, which has a primary amino acid sequence that is very similar to Kir2.1. The structural regions which are necessary for the presence or absence of an interaction of the chimeras with Kir2.1 should be restricted to the pore and C-terminal regions. This prediction was based on the already mentioned study by Tinker *et al.* [Tinker *et al.*, 1996], which defined the M2 and proximal C-terminal regions as the important regions involved in the assembly of inward rectifiers. These regions were important both for homotypic interactions and for the incompatibility between inward rectifiers from different subfamilies.

## B. Experimental Design Summary

Kir3.4 and Kir2.1 were co-expressed in *Xenopus* oocytes and the resulting currents were analyzed with respect to current level, sensitivity to extracellular [$K^+$], degree of inward rectification, and time-dependence of activation. The results were then compared with currents produced by either subunit expressed alone in an attempt to distinguish whether or not there was any interaction between the two subunits. Also, the Kir2.1 subunit was also expressed with all of the chimeric channels and analyzed in a similar fashion so as to address the question of which structural region(s) is (are) necessary for subunit interaction. In addition, in the event that there was an obvious interaction between Kir2.1 and Kir3.4, or between Kir2.1 and one of the chimeras, an assessment was made regarding which region(s), if any, dominated in conferring their characteristic properties onto the resulting heteromultimeric current.

## C. Results

### i. Co-expression of Kir2.1 with Kir3.4

#### a. Current Level

Representative current traces elicited by pulsing from -120 mV to +20 mV in 10 mV steps for Kir2.1 co-expressed with Kir3.4, along with Kir2.1 and Kir3.4 alone for comparison, are shown in Figure 4-1a. Mean I-V relationships in 40 mM KCl for Kir2.1 alone (n=15), Kir3.4 alone (n=14), and Kir2.1 co-expressed

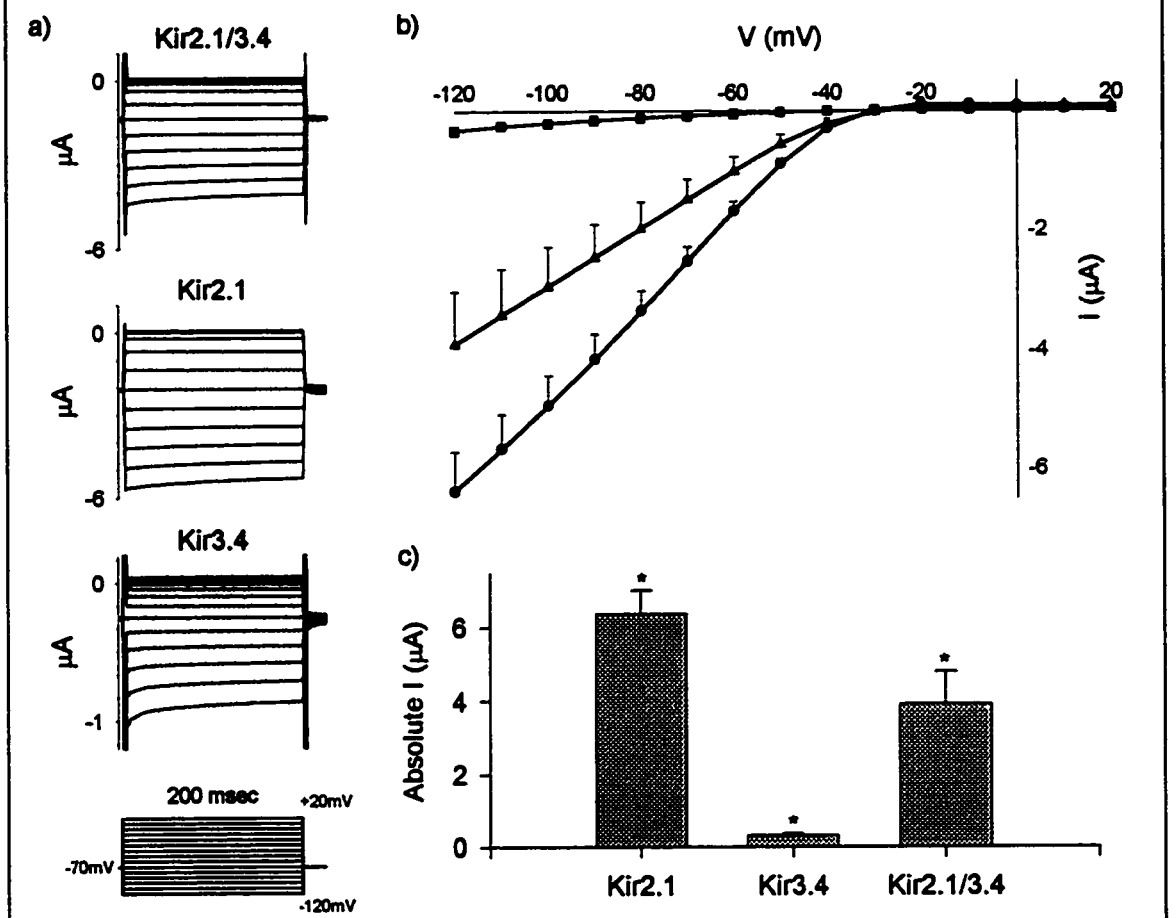


**Figure 4-1 Current Level for Kir2.1/Kir3.4** a) Representative current tracings for Kir2.1/Kir3.4 along with Kir2.1 and Kir3.4 in 40 mM KCl. Pulse protocol is shown. b) Mean I-V relationships in 40 mM KCl for Kir2.1/Kir3.4 (▲), Kir2.1 (●), and Kir3.4 (■). c) Absolute current levels at -120 mV for Kir2.1/3.4, Kir2.1, and Kir3.4. Asterisks indicate statistical significance between all three groups ($p<0.01$).

with Kir3.4 are shown in Figure 4-1b. The current levels were measured at the end of the 200 msec pulse (steady state). Absolute current levels at -120 mV in 40 mM KCl for Kir2.1 co-expressed with Kir3.4, Kir2.1 alone, and Kir3.4 alone are shown in Figure 4-1c. Statistical analysis using a One Way ANOVA and Post Hoc test showed that there was a significant difference between the current

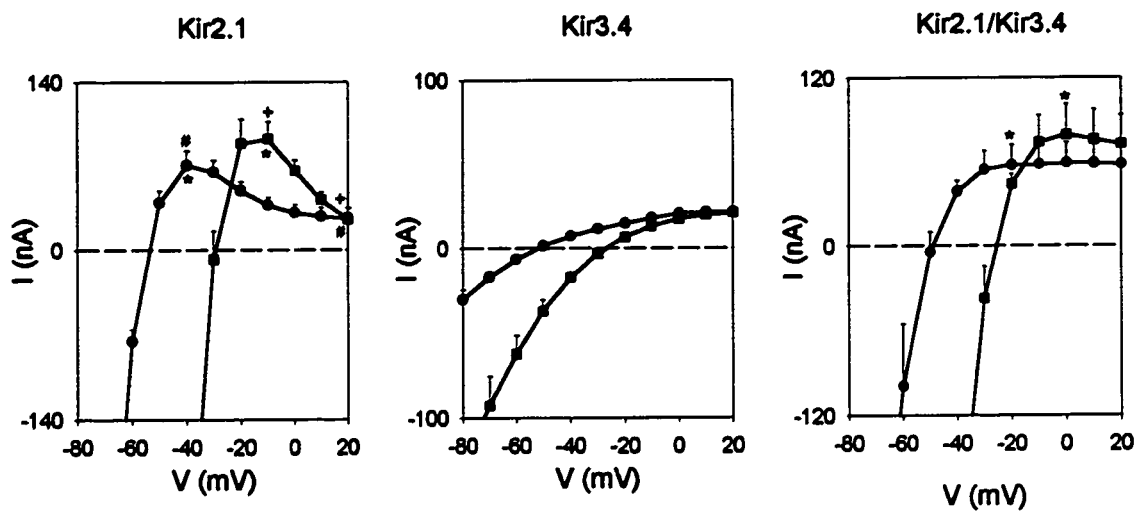


**Figure 4-2. Outward Current Comparison for Kir2.1/Kir3.4.** Mean I-V relationships for Kir2.1/Kir3.4, Kir2.1, and Kir3.4 injected oocytes in 15 (●) and 40 (■) mM KCl. Symbols indicate statistical significance between corresponding current levels ($p<0.05$).

levels for all three groups ($p<0.01$). However, the current level for Kir2.1/Kir3.4 was only 35.6% smaller than the Kir2.1 current level.

### b. $[K^+]_{out}$ Sensitivity

Figure 4-2 shows mean I-V relationships with an emphasis on the outward current in 15 and 40 mM KCl for Kir2.1/Kir3.4, Kir2.1, and Kir3.4. The co-expression current Kir2.1/Kir3.4 is qualitatively similar to Kir2.1 in that with an increase in extracellular $[K^+]$ there was an increase in outward current. Indeed, a paired t-test showed there was a significant difference between the current level at 0 mV for 40 mM KCl and at -20 mV for the 15 mM KCl current ($p<0.05$). This

is in contrast to the Kir3.4 current where there was no increase in the outward current with a corresponding increase in extracellular [$K^+$].

**c. Degree of Rectification**

Another important feature shown in Figure 4-2 is the presence or absence of a negative slope conductance. In this case, the co-expression current is more similar to Kir3.4 in that there was no statistically significant region of negative slope in the I-V relationship. The data points obtained for the condition of 40 mM extracellular [$K^+$] appeared to have a negative slope, but the difference in current levels at 0 mV and 20 mV was not statistically significant ($p>0.05$). Figure 4-3a shows the mean gK-V relationships for Kir2.1/Kir3.4, Kir2.1, and Kir3.4.

Normalization to the conductance level at -120 mV for all three groups showed that the Kir2.1/Kir3.4 group had a gKrel-V relationship with a sigmoidal appearance, which was qualitatively similar to the Kir2.1 gKrel-V relationship (Figure 4-3b). Figure 4-3c shows the single Boltzmann fit for the Kir2.1/Kir3.4 gKrel-V relationship, along with the fits for Kir2.1 and Kir3.4. The resulting fit for the co-expressed channels was similar to Kir2.1, with a $V_{½}$ of -47.3 mV and a slope factor of 14.3. These results suggest that the co-expressed current had properties that were similar to both Kir2.1 and Kir3.4. The negative slope parameter for the Kir2.1/Kir3.4 current was more similar to Kir3.4, while the opposite was true for the gKrel-V relationship, which was qualitatively and

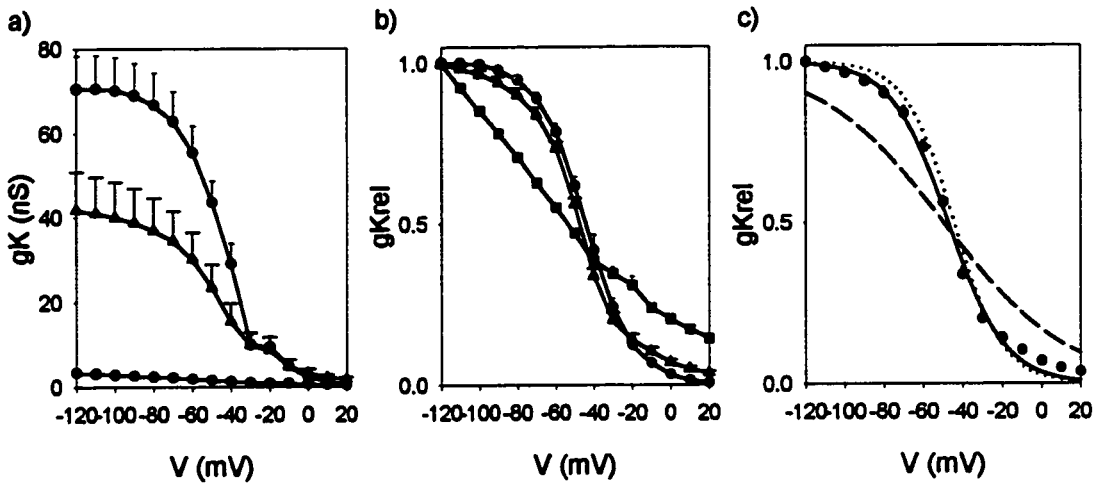


**Figure 4-3. Conductance-Voltage Relationships for Kir2.1/Kir3.4.** a) Mean gK-V relationships for Kir2.1/Kir3.4 (▲), Kir2.1(●), and Kir3.4 (■). in 40 mM KCl. b) Mean gKrel-V relationships for Kir2.1/Kir3.4, Kir2.1, and Kir3.4, same symbols apply from a). c) Boltzmann fits for Kir2.1/Kir3.4 (solid line), Kir2.1 (dotted line), and Kir3.4 (dashed line).

quantitatively similar to Kir2.1.

### d. Time-Dependence of Activation

Figure 4-4 shows representative current traces for pulses to -100 mV from a holding potential of 10 mV in 15 mM KCl for Kir2.1/Kir3.4, Kir2.1, and Kir3.4. The co-expressed current displayed an obvious time-dependent component that could be fitted with a single exponential function curve with a time constant of 2.26 ± 0.26 msec. This is comparable to the Kir2.1 time-dependence of activation of Kir2.1. The time-dependence of activation did not visually fit a double exponential which would have suggested the presence of two different populations of channels, each with a different time constant tau.

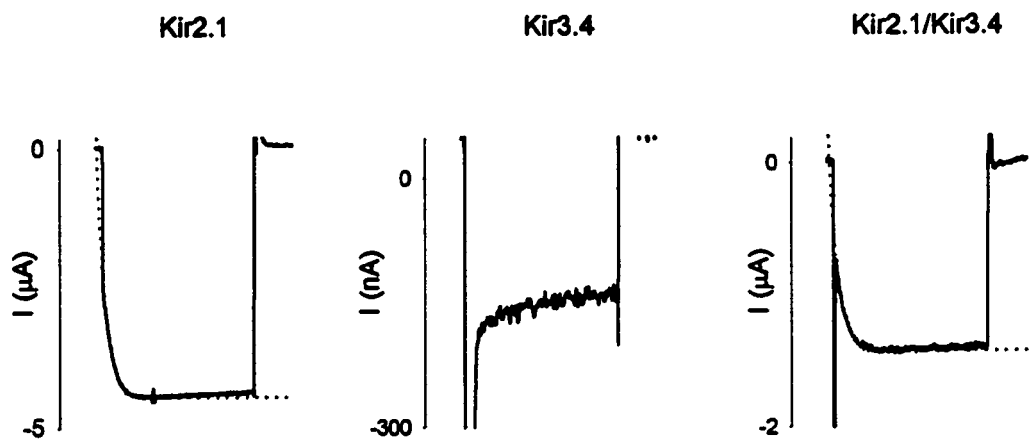


**Figure 4-4. Time-Dependence of Activation for Kir2.1/Kir3.4.** Representative current traces for 50 msec pulse to -100 mV from a holding potential of +10 mV in 15 mM KCl for Kir2.1/Kir3.4, with Kir2.1 and Kir3.4 shown for comparison. Single exponential fits for Kir2.1/3.4 shown by dashed line (tau for Kir2.1/Kir3.4 is 2.26 +/- 0.26 SEM compared to 2.19 +/- 0.18 SEM for Kir2.1).

## ii. Co-expression of Kir2.1 with Kir2.1/Kir3.4 Chimeras

### a. Current Level

Representative current traces from -120 mV to 20 mV in 10 mV steps and a holding potential of -70 mV in 40 mM KCl for Kir2.1 co-expressed with all six chimeras are shown in Figure 4-5. Figure 4-6a shows the mean I-V relationships in 40 mM KCl for Kir2.1 alone and when co-expressed with all six chimeras. A bar graph showing the absolute current levels at -120 mV for Kir2.1 alone, when co-expressed with a particular chimera, and that chimera alone is shown in Figure 4-6b. Statistically significant differences were determined by a One Way ANOVA and Post Hoc test ($p<0.01$). Specific differences between

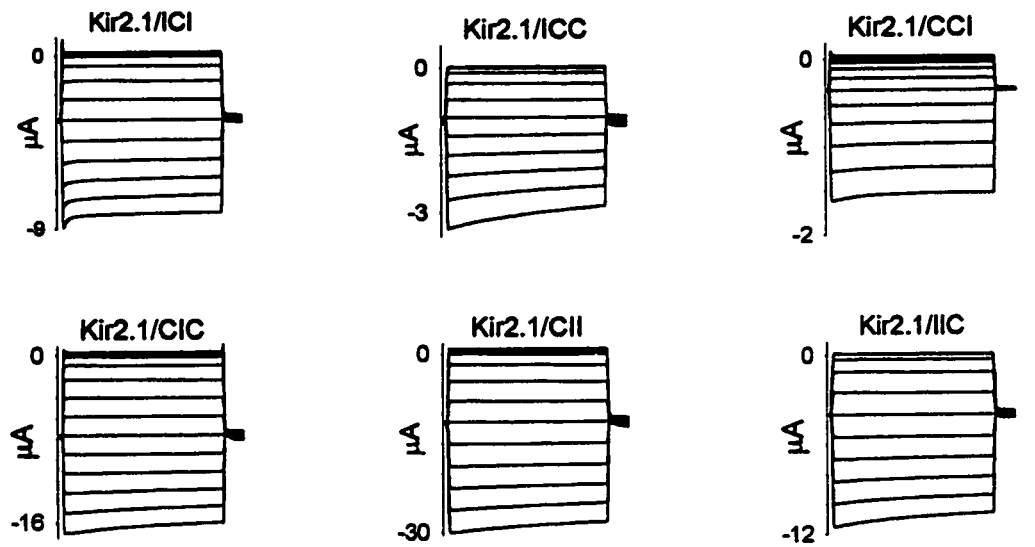


**Figure 4-5. Representative Kir2.1/Chimera Co-Expression Currents.** Representative current traces for Kir2.1 when co-expressed with ICI, ICC, CCI, CIC, CII, or IIC in 40 mM KCl. Pulse protocol is same as previous.

groups are indicated by corresponding symbols. For the ICI chimera, it appeared that there was a negative interaction with Kir2.1 in that the current level for the co-expression is intermediate between that of either expressed individually. The co-expression current could not be explained by the simple summation of both individual currents. For both the ICC and IIC chimeras, there appeared to be no interaction as there was no statistical difference between the current levels for Kir2.1 alone and when expressed with either ICC or IIC. Neither of these chimeras express on their own. The CCI chimera expresses current when expressed on its own, but also showed a dominant-negative

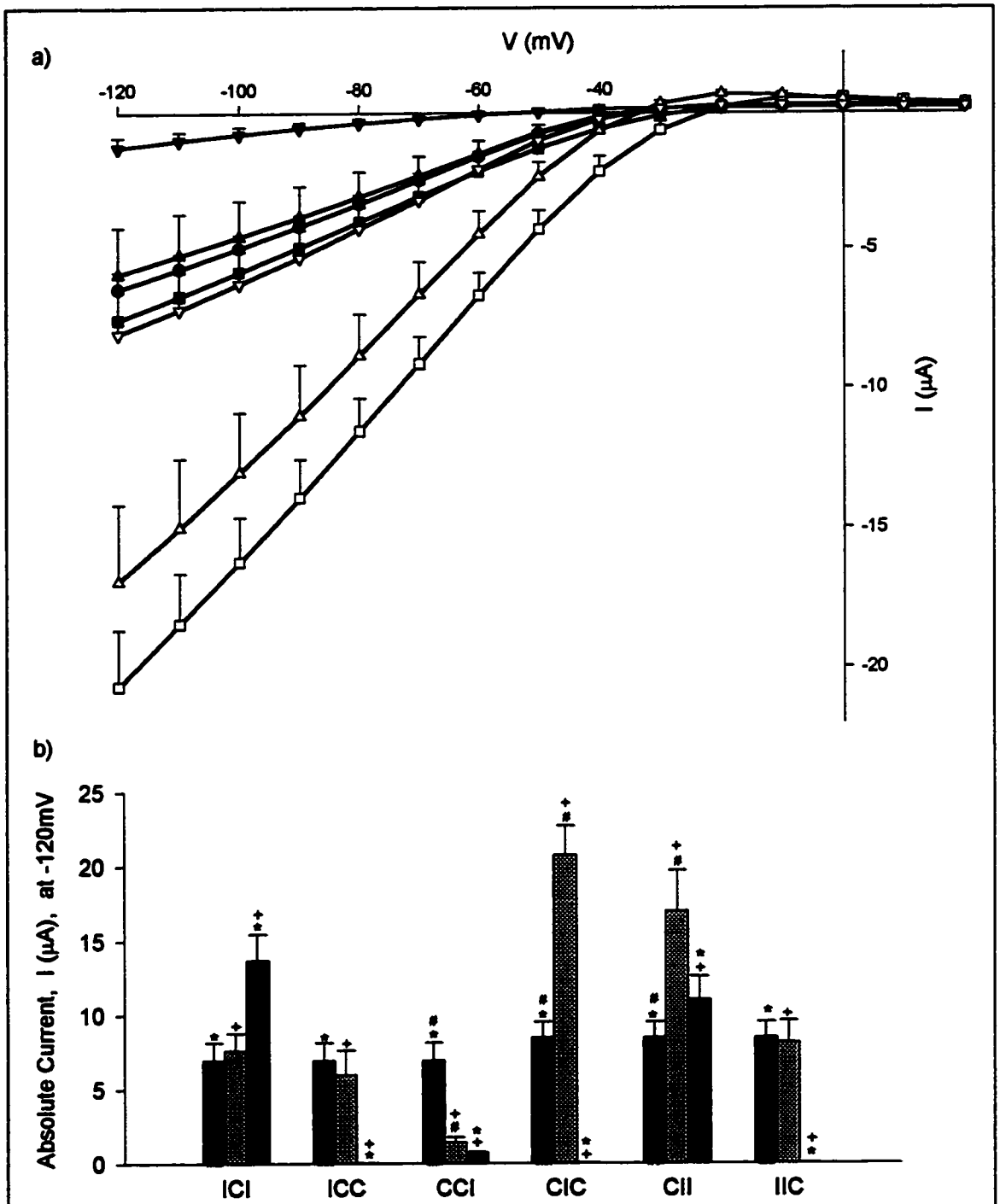


**Figure 4-6. Current Levels for Kir2.1/Chimera Co-Expression Currents.** a) Mean I-V relationships for Kir2.1 when expressed alone (●, n=9), and when expressed with ICI (■, n=9), ICC (▲, n=6), CCI (▼, n=7), CIC (□, n=5), CII (△, n=6), and IIC (▽, n=6) in 40 mM KCl. b) Bar graph showing absolute current levels at -120 mV for Kir2.1 alone, when expressed with a particular chimera, and that chimera alone. Statistical significance between current levels is indicated by corresponding symbols ($p<0.01$).

effect on Kir2.1 because the co-expressed current was significantly smaller than the Kir2.1 current. Another interesting result is the CIC chimera which alone produces no current, but when expressed with Kir2.1 shows a significant positive interaction. There is significant increase in the co-expression current with CIC when compared to Kir2.1 alone. It seems that Kir2.1 has the ability to rescue the non-expressing CIC chimera. The final chimera is the CII chimera which when coexpressed with Kir2.1 shows a large current that could be explained either by simple summation of the two individual currents, or could include functional heteromultimers that display electrophysiological properties that are indistinguishable from homomultimeric Kir2.1 and CII channels.

**b. $[K^+]_{out}$ Sensitivity**

Figure 4-7 shows mean I-V relationships with an emphasis on the outward current in both 15 and 40 mM KCl for Kir2.1 co-expressed with all six chimeric channels. In all cases, except the co-expression of Kir2.1 with CCI, there is a qualitative similarity to the individually expressed Kir2.1 current with respect to sensitivity to extracellular $[K^+]$. Of these five chimeras, four of them show a statistically significant increase in the outward current with an increase in extracellular $[K^+]$ That is, the current level in 40 mM KCl at -10 mV was significantly higher than the current level at -30 mV in 15 mM KCl. The Kir2.1/ICI co-expression current did not show a statistically significant difference for the outward currents. The remaining co-expression current, Kir2.1/CCI,

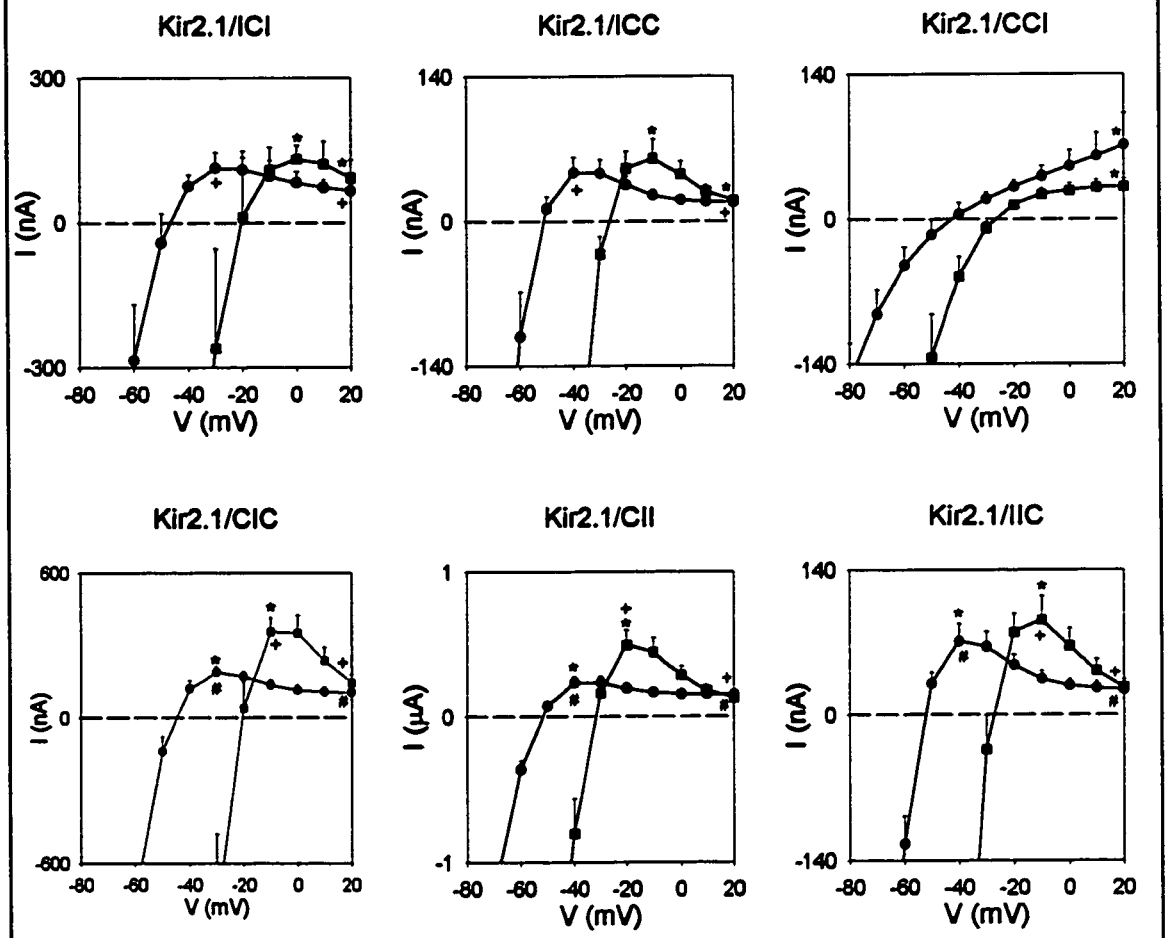


**Figure 4-7. Outward Current Comparisons for Kir2.1/Chimera Co-Expression Currents.** Mean I-V relationships for all the Kir2.1/chimera co-expression currents, with a focus on the outward current. Symbols indicate statistical significance between corresponding current levels ($p<0.05$).

qualitatively shows a decrease in the outward current which was statistically significant ($p<0.05$).

### c. Degree of Rectification

With respect to presence or absence of negative slope, it may be seen in Figure 4-7 that all co-expression currents, with the exception of Kir2.1/CCI,

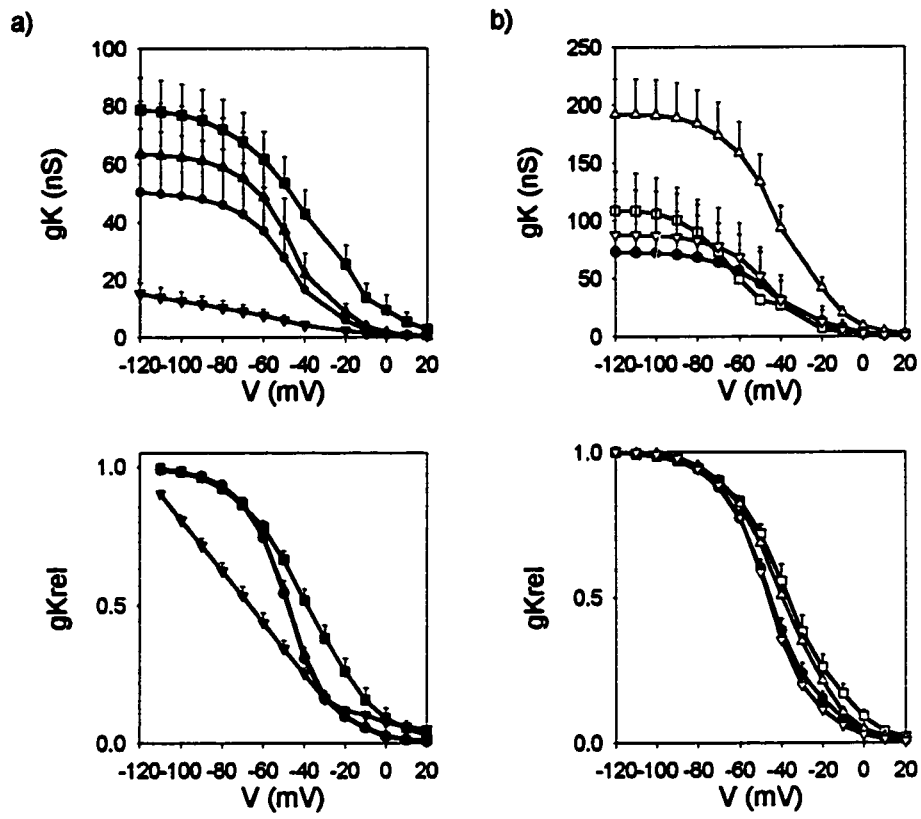


**Figure 4-8. Conductance-Voltage Relationships for Kir2.1/Chimera Co-Expression Currents.** a) Mean gK-V relationships for all of the Kir2.1/chimera co-expression currents in 40 mM KCl. b) Mean gKrel-V relationships for the Kir2.1/chimera co-expression currents in 40 mM KCl. Kir2.1 alone (●), with ICI(■), ICC(▲), CCI(▼), CIC(□), CII(△), and IIC(▽). Relationships are separated into Kir3.4 pore based chimeras (left) and Kir2.1 based (right) for clarity.

showed a significant region of negative slope conductance. All five show a statistical difference in the current level at -30 mV or -10 mV for 15 and 40 mM KCl, respectively, and the current level at 20 mV. However, Kir2.1/CCI showed no evidence of a region of negative slope conductance. These results are in general agreement with the results with respect to extracellular [$K^+$] sensitivity.

Figure 4-8a shows the gK-V relationships for Kir2.1 alone and co-expressed with the six chimeric channels. Figure 4-8b shows the normalized

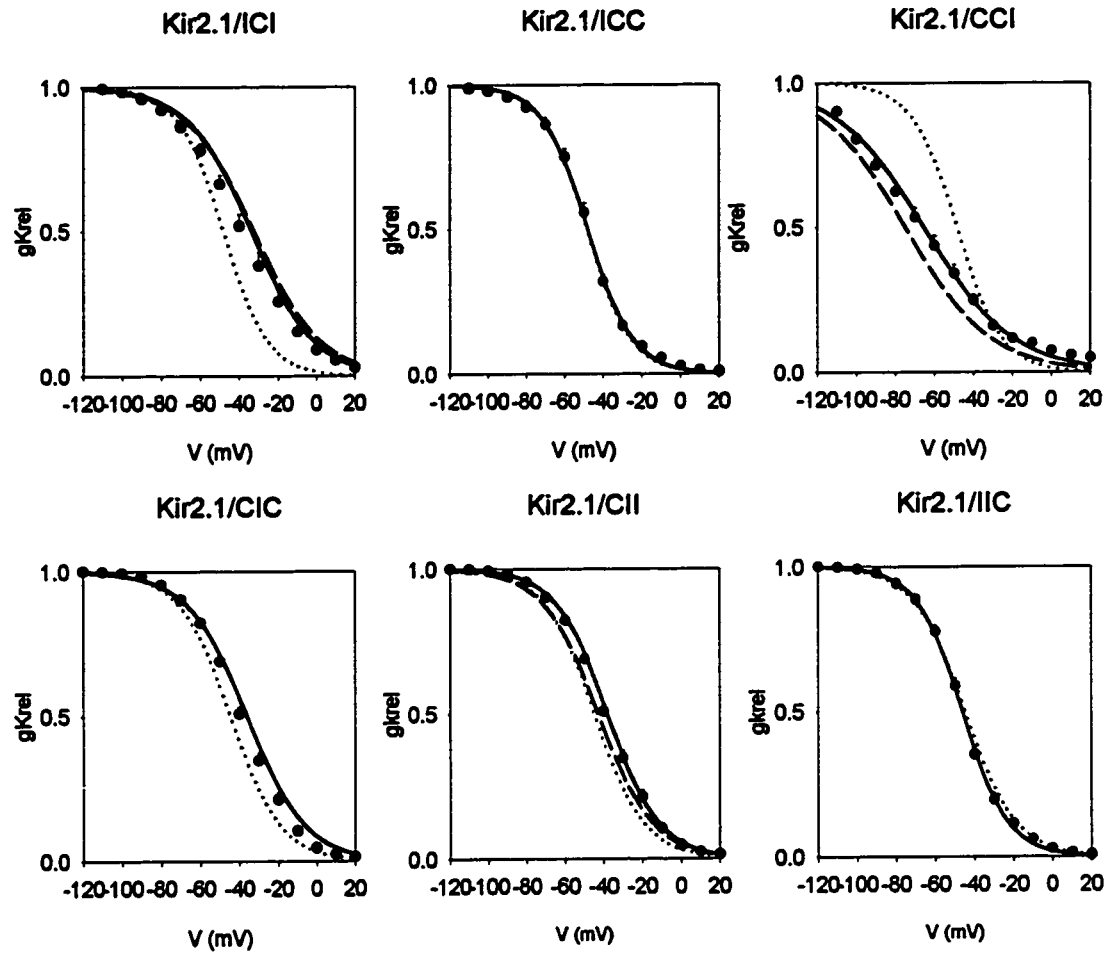


**Figure 4-9. Boltzmann Fits for the Kir2.1/Chimera Co-Expression Currents.** For each gKrel-V relationship the Boltzmann fit is shown for the corresponding co-expression current (solid line), along with the fits for the Kir2.1 current (dotted line) and the individually expressed chimeric channel if applicable (dashed line).

gKrel-V relationships for the same currents. Again, all of the co-expression currents, except the Kir2.1/CCI current, showed a gKrel-V relationship that was similar to the Kir2.1 current in that they could be fitted by a sigmoidal curve. The Kir2.1/CCI is very similar to the gKrel-V relationship for the CCI current alone. The Boltzmann fits for all of the co-expression currents are shown in Figure 4-9.

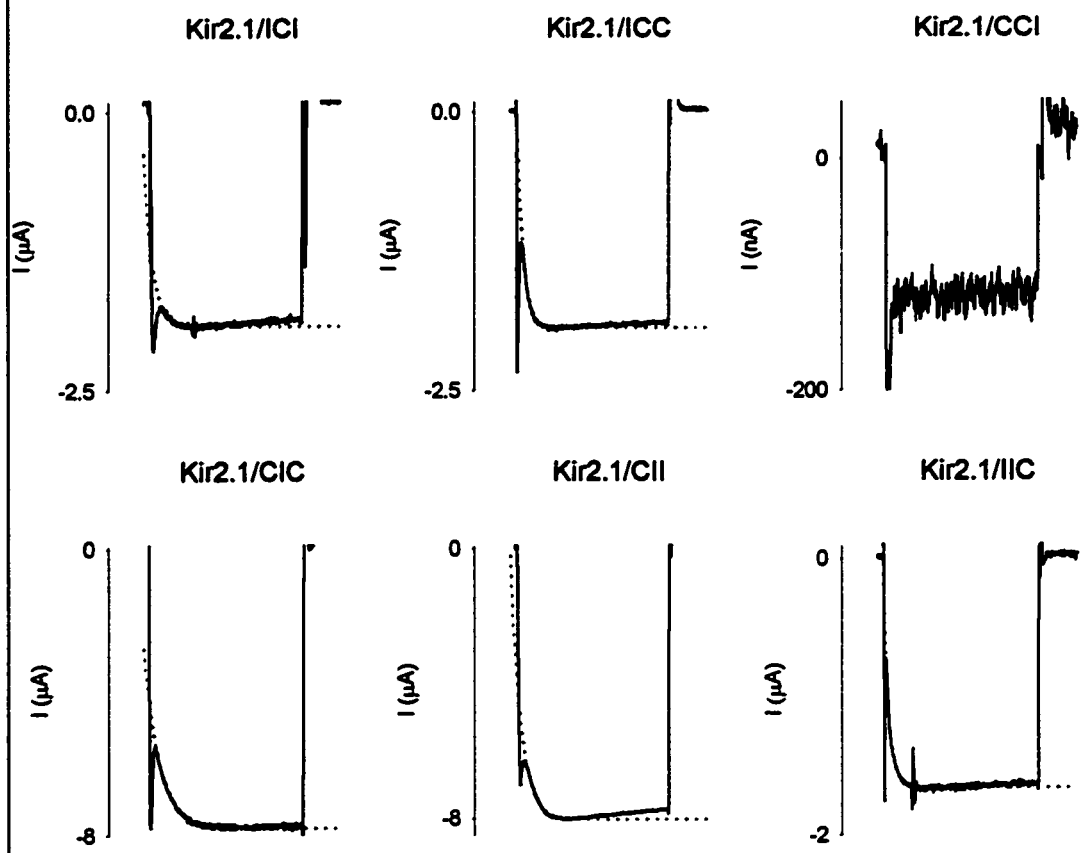


**Figure 4-10. Time-Dependence of Activation for Kir2.1/Chimera Co-Expression Currents.** Representative current traces for 50 msec pulses to -100 mV from a holding potential of +10 mV in 15 mM KCl for all the Kir2.1/chimera co-expression currents. With the exception of the Kir2.1/CCI current, all co-expression currents could be fit with a single exponential fit, shown as dashed line.

The $V_{½}$ values and slope factors are listed in Table 4-1 later in this chapter. These results suggest that all of the co-expression currents show a rectification that is similar to Kir2.1, but the Kir2.1/CCI current appears to be rectified or has an inactivation that is entirely different than Kir2.1 and the other co-expression currents.

### d. Time-Dependence of Activation

Figure 4-10 shows representative current traces elicited by pulses to -100 mV from a holding potential of 10 mV, in 15 mM KCl, for all of the co-expression currents. The same pattern is being displayed in that all of them, except the Kir2.1/CCI current, show time-dependence of activation. The taus for the co-expression currents are as follows: Kir2.1 with ICI was 2.02 ± 0.35 msec, with ICC 1.4 ± 0.37 msec, with CIC 2.11 ± 0.37msec, with CII 3.18 ± 0.25 msec, and with IIC 1.77 ± 0.16 msec. It appears from all of these results that the CCI chimera has the ability to interact with Kir2.1 and subsequently confer its properties in a dominant way onto the resulting current.

## D. Discussion

A summary of the results for Study Two is shown in Table 4-1. In order to determine the presence of an obvious interaction between co-expressed subunits, the resulting current level should not be explained by a simple summation of the current levels produced when either subunit is expressed individually. Also, the presence of any functional heteromultimeric channel could only be concluded if the resulting electrophysiological properties were significantly different from either homomultimeric current. In the case of Kir2.1 co-expressed with Kir3.4, the results are unclear, however, the co-expression of Kir2.1 with the chimeric channels is more straightforward with respect to determining the presence or absence of an interaction.

**Table 4-1. Summary of Results for Study Two.** The current level parameter is a comparison to the current level for Kir2.1 when expressed alone. The gKrel-V relationships were fit to a single Boltzmann and the corresponding $V_{1/2}$ and slope factor are shown.

| Channel | Current Level | Sensitivity to $[K]_{out}$ | Negative Slope | gKrel-V | Time Dependence |
|---|---|---|---|---|---|
| Wild Type | | | | | |
| Kir2.1 | high | increase | yes | -44.6mv, 12.6 | yes |
| + Kir3.4 | slight decrease | increase | yes | -47.4mV, 15.5 | yes |
| Chimeras | | | | | |
| + ICI | slight increase | no change | yes | -38.4mV, 16.9 | yes |
| + ICC | no change | increase | yes | -48.0mV, 11.8 | yes |
| + CCI | sig. decrease | no change | no | no fit | no |
| + CIC | sig. increase | increase | yes | -36.2 mV, 15.2 | yes |
| + CII | sig. increase | increase | yes | -39.1mV, 13.8 | yes |
| + IIC | slight increase | increase | yes | -46.1mV, 11.7 | yes |

Two of the co-expression currents showed that there was no obvious interaction between the particular chimera and Kir2.1. The chimeras for these experiments were ICC and IIC, both of which do not express current on their own and neither have any effect on the current level of Kir2.1. Both of these chimeras contain the C-terminal region of Kir3.4, which is, according to Tinker

and co-workers [Tinker *et al.*, 1996] one of the important regions for incompatibility between subfamilies. Interestingly, the other chimera with a Kir3.4 C-terminal region, CIC, which also does not express on its own, had a synergistic effect on Kir2.1. That is, the co-expression current was almost three times larger than Kir2.1 current. It seems that the compatible pore regions between Kir2.1 and CIC are enough to rescue the non-expressing chimera. So what does this say about the CIC chimera and its inability to form a functional channel on its own? There are several possibilities: the CIC subunits cannot assemble into a functional channel on their own, the CIC subunits form a tetrameric channel that is non-conducting or permanently inactivated, or the CIC subunits form a tetramer that lacks the appropriate signal necessary for transport to the cell membrane. In any event, there is an interaction with Kir2.1 that counteracts any mechanism that prevents CIC subunits from producing a measureable current. This interaction, between Kir2.1 and CIC, is the only unambiguous evidence in this study that suggests the formation of a functional heteromultimer.

Co-expression of Kir2.1 with the CII chimera resulted in a huge current that had properties that were almost identical to either Kir2.1 or CII when expressed alone. The resulting current could be explained either by the summation of the individual homomeric currents, or could involve a heteromultimer with properties similar to both Kir2.1 and CII. Of the remaining chimeras, both exhibited current levels that were intermediate in amplitude

compared to the individual currents. The individual ICI current was quite large but when expressed with the Kir2.1 channel the resulting current was smaller. Since ICI contains the C-terminal of Kir2.1, it had the ability to interact with wild type Kir2.1 subunits, but the incompatibility between the pore regions of Kir2.1 and Kir3.4, which is present in the ICI chimera, would seem to be sufficient that any resulting interaction produces a channel with significantly changed conductance properties or a non-functional complex that is not inserted into the membrane. Only 9% of the RNA injected is contributed by Kir2.1 while the other 90% is of ICI origin. If you assume that interaction follows a binomial distribution, then after being translated Kir2.1 subunits have a greater probability of interacting with an ICI subunit, which has compatible C-terminal regions, to form a non-viable complex. As a result, very few homomultimeric Kir2.1 channels are formed. The end result was a current that displayed properties more similar to ICI, as it dominated due to the greater density of homomultimeric channels.

The only remaining chimera which has not been discussed is the CCI chimera which produced another interesting result. The co-expression of CCI with Kir2.1 produced a low level current with a non-saturating conductance typical of individually expressed CCI subunits. There are two possible explanations for this observation: first, the resulting current is represented by a population of channels that are dominated by CCI homomultimers. Any interaction between Kir2.1 and CCI resulted in a non-viable complex that does

not contribute to the overall current. Second, there is a heteromultimer formed between Kir2.1 and CCI whereby the inactivation mechanism of CCI dominated in the resulting channel. It is possible that these two subunits can form a channel and that the inclusion of one or more CCI subunits is enough to confer the intrinsic inactivation property, discussed in Chapter 3, to the heteromultimer. At the very least there is an interaction which can be explained by the fact that the C-terminal region of Kir2.1 is present on the CCI chimera. Whether or not there was any functional heteromultimer was indeterminable. The properties of negative slope, sensitivity to extracellular [$K^+$], sigmoidal gKrel-V relationship, and time-dependent activation are absent from the co-expression current. Considering that CCI was injected at ten times the concentration it is not surprising, however, because the simple inclusion of an intrinsic inactivation on any heteromultimeric channel would confer the same absence of these properties.

With respect to the results for co-expression of Kir2.1 with Kir3.4, the data from the present study could not unambiguously define whether there is an interaction between the subunits, or whether functional heteromultimers between Kir2.1 and Kir3.4 were formed. The current level for the Kir2.1/Kir3.4 co-expression is approximately 35% smaller than the individually expressed Kir2.1 channel, while the remaining electrophysiological properties are very similar to Kir2.1. That is, the Kir2.1/Kir3.4 co-expression current shows sensitivity to extracellular [K+], a sigmoidal conductance-voltage relationship, and time-

dependent activation. The only characteristic property of Kir2.1 that is missing in the co-expression of Kir2.1 and Kir3.4 was a statistically significant negative slope conductance. This can be explained by the overlap and summation of outward currents produced by Kir2.1 and Kir3.4 homomultimers. The outward current of Kir3.4 shows no negative slope and if you add it to the outward current of Kir2.1 the effect would be to minimize the overall presence of negative slope to the point where it is no longer statistically significant.

The original hypothesis was that Kir2.1 and Kir3.4 would either not interact or Kir3.4 would exert a dominant-negative effect on Kir2.1. The dominant-negative effect means that Kir3.4 would dominate by knocking out the current produced by Kir2.1. If the assembly of inward rectifier subunits into functional channels followed the rules of a binomial distribution, then injecting ten times more RNA of the subunit that is supposed to knock out the other should completely abolish the current. In the case of Kir2.1 and Kir3.4 the resulting current is only about 35% smaller than the Kir2.1 current. This suggests that Kir3.4 does not interact with Kir2.1. In fact, the reduction in current amplitude may also reflect an overload of RNA and lack of expression. It is possible the oocyte cannot process the RNA fast enough and is tied up translating the RNA for Kir3.4, which is in excess; thereby reducing the quantity of Kir2.1 RNAs that are translated. Further evidence supporting this notion is that the resulting current displays the properties of the Kir2.1 current that are associated with inward rectification.

To summarize, the results obtained suggest that an interaction between Kir2.1 and Kir3.4 is either extremely weak or does not occur. This conclusion was supported by the fact that a ten fold excess of Kir3.4 RNA had only a 35% reduction in the current level when compared to individually expressed Kir2.1 channels. Interactions between Kir2.1 and the chimeras appeared to be confined to chimeras that contained either the pore or C-terminal regions of Kir2.1. However, the presence of any heteromultimeric channel could not be confirmed unless the resulting co-expression current was strikingly different than either of the currents produced when the subunits are expressed separately. The only chimera to demonstrate this striking difference was the CIC chimera, which on its own produced no current, but managed to triple the current amplitude when co-expressed with Kir2.1, compared to individually expressed Kir2.1 channels.

For the remaining chimeras, the only conclusions that could be reached with any degree of confidence were those that stated the presence or absence of an interaction. First, there was no interaction, either positive or negative, between Kir2.1 and the ICC and IIC chimeras. Second, negative interactions occurred between Kir2.1 and the chimeras ICI and CCI as the resulting current levels were intermediate to the current levels produced by these subunits when individually expressed. Finally, the CII chimera showed no obvious interaction with Kir2.1, although an interaction would have been difficult to detect

considering the striking similarity in the electrophysiological properties of the two channels.

## Chapter 5: Conclusions

The experiments in this thesis were designed with the following questions in mind:

* How do the currents produced by the mouse Kir3.4 clone isolated in our lab compare to the currents from the mouse Kir2.1 clone, when injected into *Xenopus* oocytes, with respect to expression levels and the properties of extracellular [$K^+$] sensitivity, negative slope conductance, saturating conductance-voltage relationships, and time-dependent activation?
* What general structural regions of Kir3.4 or Kir2.1, confer these properties to the resulting current? The structural regions were separated into the N-terminal, pore, and C-terminal regions.
* Do the mouse Kir2.1 and Kir3.4 clones interact in any way when co-expressed together in *Xenopus* oocytes, where an interaction would be described as a resulting current that could not be explained by the simple summation of the two individual currents?
* What general structural regions of Kir2.1 or Kir3.4 allow or prevent any interaction between these two channels?

The first question was addressed in Study One with the results showing that the Kir3.4 current yields a much lower level of expression than Kir2.1. Also,

the properties of extracellular [$K^+$] sensitivity, negative slope conductance, saturation of the conductance-voltage relationship at -120 mV, and time-dependent activation were demonstrated in the Kir2.1 currents but were not evident in the Kir3.4 currents. The lack of saturation in the conductance-voltage relationship for Kir3.4 and the fact that it is part of the subfamily that is regulated by G proteins suggests that Kir3.4 may exhibit an inactivation mechanism. The presence of this mechanism can explain the low current level and the additional properties which may be attributed to inward rectification.

The second question was also addressed in Study One with the results showing that the property of a low non-saturating conductance current characteristic of Kir3.4 was conferred by the N-terminal and pore regions. Also, the inward rectification properties were associated with large current levels which appeared to be restricted to channels that contain the C-terminal region of Kir2.1 that was paired with alternating Kir2.1 and Kir3.4 N-terminal and pore regions. As long as either the N-terminal or the pore region of Kir2.1 were present, then large current levels were seen that displayed the properties of extracellular [$K^+$] sensitivity, negative slope conductance, saturation of conductance-voltage relationship, and time-dependent activation. Finally, the C-terminal region of Kir3.4 appears to be compatible only with the N-terminal and pore regions from Kir3.4 as all of the chimeras constructed with the Kir3.4 C-terminal region failed to express.

The third question was addressed in Study Two with the results suggesting that Kir2.1 and Kir3.4 either show a weak or non-existent interaction. The reason for this conclusion was based on the fact that the co-expression current could be explained either by a weak negative interaction or by an overload of RNA.

The final question was also addressed in Study Two with the results showing consistency with results obtained by Tinker *et al.*[Tinker *et al.*, 1996]. That is, the M2 and C-terminal regions are most important with respect to interactions between identical and different subunits. Two of the chimeric channels that contained the C-terminal region of Kir3.4, IIC and ICC, failed to show any interaction with Kir2.1. The remaining chimera with a Kir3.4 C-terminus, CIC, produced a synergistic effect on Kir2.1 which could be explained by the presence of the M2 region of Kir2.1 in CIC. Of the chimeras with the Kir2.1 C-terminal region, only CII did not show any obvious interaction, although any interaction would have been difficult to observe because properties between Kir2.1 and CII are almost identical. The ICI chimera interacted in a negative fashion on Kir2.1. The interaction was probably due to the compatible C-terminal regions, but no current was produced because of incompatible pore regions. The final chimera, CCI, also interacted with Kir2.1 in a negative fashion, with the resulting current being similar to CCI. The interaction is either a dominant-negative effect of CCI on Kir2.1 or the two co-assemble to form a

heteromultimer where the CCI subunits confer their properties on to the resulting current.

In conclusion, the results here would be more convincing with additional studies. Some experiments that might add more insight would involve single channel analysis, immunofluorescence to determine cell surface expression, co-expression with Gβγ subunits to examine fully activated Kir3.4 and CCI currents, and the use of dominant-negative mutants for co-expression with Kir2.1. More specifically, the question as to why the Kir3.4 currents are smaller needs to be addressed. The model presented in Chapter 3 suggested that Kir3.4 is not subjected to rectification by pore block, rather, this channel displays an inactivation mechanism that is intrinsic to the protein itself. In any event, studies aimed at characterizing the Kir3.4 conductance properties may shed some light on why this channel shows a low-level current with a conductance-voltage relationship that does not saturate at -120 mV. Immunofluorescence studies could determine if the low level of current is due to lack of sufficient cell surface expression. Single channel analysis, whereby the concentrations of polyamines and $Mg^{++}$ could be manipulated, could be used to determine Kir3.4 conductance properties, including the degree of rectification due to intracellular pore block. Experiments involving co-expression of Gβγ subunits could be used to examine the fully activated Kir3.4 channels, assuming of course that Gβγ does fully activate the channel.

With respect to the co-expression studies, the presence or absence of any functional heteromultimers was, except for Kir2.1/ClC, indeterminable. The use of AAA dominant-negative constructs, as utilized by the Jan laboratory [Tinker *et al.*, 1996], may provide more insight as to whether or not any heteromultimers were formed. The presence of AAA, instead of GYG, in one of the four subunits required to form a functional tetramer results in a non-conducting channel. For example, for the co-expression Kir2.1/CCl it was unclear whether the resulting current was composed mainly of CCl homomultimers or contained some heteromultimers where CCl conferred its properties onto the resulting channel. The use of Kir2.1-AAA dominant-negative mutant in the co-expression should have no effect on the current if no heteromultimers are formed, while the use of CCl-AAA should almost completely abolish the current. In any event, future studies would be required before any conclusions could be made regarding the presence or absence of any functional heteromultimers.

**References**

Ashcroft, FM. 1988. Adenosine 5-triphosphate-sensitive potassium channels. *Annu. Rev. Neurosci.* **11**:97-118.

Ashford, MLJ., Bond, CT., Blair, TA., and Adelman, JP. 1994. Cloning and functional expression of a rat heart $K_{ATP}$ channel. *Nature* **370**:456-459.

Biermans, G., Vereecke, J., and Carmeliet, E. 1987. The mechanism of the inactivation of the inward-rectifying K current during hyperpolarizing steps in guinea-pig ventricular myocytes. *Pflügers Arch.* **410**:604-13.

Brown, AM. 1993. Functional bases for interpreting amino acid sequences of voltage-dependent $K^+$ channels. *Annu. Rev. Biophys. Biomolec. Struct.* **22**:173-198.

Chan, KW., Langan, MN., Sui, JL., Kozak, JA., Pabon, A., Ladias, J., Logothetis, DE. 1996. A recombinant inwardly rectifying potassium channel coupled to GTP-binding proteins. *J. Gen. Physiol.* **107**:381-397.

Cole, WC., McPherson, CD., and Sontag, D. 1991. ATP-regulated $K^+$ channels protect the myocardium against ischemia-reperfusion damage. *Circ. Res.* **69**:571-581.

Cole, WC., and Aeillo, EA. 1994. Therapeutic modulation of ATP sensitive potassium channels in ischaemia [letter: comment]. *Cardiovasc. Res.* **28(2)**:286-7.

Dascal, N., Doupnik, CA., Ivanina, T., Bausch, S., Wang, W., Lin, C., Garvey, J., Chavkin, C., Lester, HA., and Davidson, N. 1995. Inhibition of function in *Xenopus* oocytes of the inwardly rectifying G-protein-activated atrial K channel (GIRK1) by overexpression of a membrane-attached form of the C-terminal tail. *Proc. Natl. Acad. Sci. U.S.A.* **92**:6758-6762.

DiFrancesco, D., Ferroni, A., and Viscentin, S. 1984. Barium-induced blockade of the inward rectifier in calf Purkinje fibers. *Pflügers Arch.* 402:446-453.

Doupnik, CA., Davidson, N., and Lester, HA. 1995. The inward rectifier potassium channel family. *Curr. Opin. Neurobiol.* **5**:268-277.

Fakler, B., Brandle, U., Bond, C., Glowatzki, E., Koening, C., Adelman, JP., Zenner, HP., and Ruppersberg, JP. 1994. A structural determinant of

differential sensitivity of cloned inward rectifier $K^+$ channels to intracellular spermine. *FEBS Lett.* **356**:199-203.

Ficker, E., Taglialatela, M., Wible, BA., Henley, CM., and Brown, AM. 1994. Spermine and spermidine as gating molecules for inward rectifier $K^+$ channels. *Science* **266**:1068-1072.

Fink, M., Duprat, F., Heurteaux, C., Lesage, F., Romey, G., Barhanin, J., and Lazdunski, M. 1996. Dominant-negative chimeras provide evidence for homo and heteromultimeric assembly of inward rectifier $K^+$ channel proteins via their N-terminal end. *FEBS Lett.* **378**:64-68.

Giles, WR., and Imaizumi, Y. 1988. Comparison of potassium currents in rabbit atrial and ventricular cells. *J. Physiol.* **405**:123-145.

Glowatzki, E., Fakler, G., Brändle,U., Rexhausen, U., Zenner, H.P., Ruppersberg, JP., and Fakler, B. 1995. Subunit-dependent assembly of inward rectifier $K^+$ channels. *Proc. R. Soc. Lond.* **261**:251-261.

Guardobasso, V., Munson, PJ., and Rodbard, D. 1988. A versatile method for simultaneous analysis of families of curves. *FASEB J.* **2**:209-215.

Hedin, KE., Lim, NF., and Clapham, DE. 1996. Cloning of a *Xenopus laevis* inwardly rectifying $K^+$ channel subunit that permits GIRK1 expression of $I_{KACh}$ currents in oocytes. *Neuron* **16**:423-429.

Heidbüchel, H., Vereecke, J., and Carmeliet, E. 1987. The electrophysiological effects of acetylcholine in single human atrial cells. *J. Mol. Cell. Cardiol.* **19**:1207-1219.

Heidbüchel, H., Vereecke, J., and Carmeliet, E. 1990. Three different potassium channels in human atrium: Contribution to the basal potassium conductance. *Circ. Res.* **66**:1277-1286.

Ho, K., Nichols, CG., Lederer, WJ., Lytton, J., Vassilev, PM., Kanazirska, MV., and Hebert, SC. Cloning and expression of an inwardly rectifying ATP-regulated potassium channel. *Nature* **362**:31-38.

Hille, B. 1992. Chapter 5. Potassium Channels and Chloride Channels. In *Ionic Channels of Excitable Membranes.* Sinauer Associates, Inc. Sunderland, Massachusetts. pp115-139.

Hille, B., and Schwarz, W. 1978. Potassium channels as multi-ion single-file pores. *J. Gen. Physiol.* **72**:409-442.

Huang, C., Jan, YN., and Jan, LY. 1997. Binding of the G protein βγ subunit to multiple regions of G protein-gated inward-rectifying $K^+$ channels. *FEBS Lett.* **405**:291-298.

Hume, JR., and Uehara, A. 1985. Ionic basis of the different action potential configurations of single guinea-pig atrial and ventricular myocytes. *J. Physiol.* **268**:525-544.

Ibarra, J., Morley, GE., and Delmar, M. 1991. Dynamics of the inward rectifier $K^+$ current during the action potential of guinea pig ventricular myocytes. *Biophys. J.* **60**:1534-1539.

Iizuka, M., Kubo, Y., Tsunenari, I., Pan, CX., Akiba, I., and Kono, T. 1995. Functional characterization and localization of a cardiac-type inwardly rectifying $K^+$ channel. *Recept. and Chann.* **3**:299-315.

Inagaki, N., Tsuura, Y., Namba, N., Masuda, K., Gonoi, T., Horie, M., Seino, Y., Misuta, M., and Seino, S. 1995a. Cloning and functional characterization of a novel ATP-sensitive potassium channel ubiquitously expressed in rat tissues, including pancreatic islets, pituitary, skeletal muscle, and heart. *J. Biol. Chem.* **270**:5691-5694.

Inagaki, N., Gonoi, T., Clement IV, JP., Namba, N., Inazawa, J., Gonzalez, G., Aguilar-Bryan, L., Seino, S., and Bryan, J. 1995b. Reconstitution of $I_{KATP}$: an inward rectifier subunit plus the Sulfonylurea Receptor. *Science* **270**:1176-1170.

Irisawa, H., Nakayama, T., and Noma, A. 1987. Membrane currents of single pacemaker cells from rabbit S-A and A-V nodes. In *Electrophysiology of Single Cardiac Cells.* Noble, D., and Powell, T. eds.. Academic Press, London. pp 167-186.

Isenberg, G. 1976. Cardiac Purkinje fibers: Cesium as a tool to block inward rectifying potassium currents. *Pflügers Arch.* **391**:85-100.

Ishihara, K., and Hiraoka, M. 1994. Gating mechanism of the cloned inward rectifier potassium channel from mouse heart. *J. Membr. Biol.* **142**:55-64.

Lopatin, AN., Mahkina, EN., and Nichols, CG. 1994. Potassium channel block by cytoplasmic polyamines as the mechanism of intrinsic rectification. *Nature* **372**:366-369.

Lopatin, AN., and Nichols, CG. 1996. [$K^+$] dependence of polyamine-induced rectification in inward rectifier potassium channels (Irk1, Kir2.1). *J. Gen. Physiol.* **108**:105-113.

Jan, LY., and Jan, YN. 1992. Structural elements involved in specific $K^+$ channel functions. *Ann. Rev. Physiol.* **54**:537-555.

Katz, B. 1949. Les constantes électriques de la membrane du muscle. *Arch Sci Physiol.* **3**:285-299.

Kennedy, ME., Nemec, J., and Clapham, DE. 1996. Localization and interaction of epitope-tagged GIRK1 and CIR inward rectifier $K^+$ channel subunits. *Neuropharmacology* **35**:831-839.

Krapivinsky, G., Gordon, EA., Wickman, K., Velimirovic, B., Krapivinsky, L., and Clapham, DE. 1995a. The G-protein-gated atrial $K^+$ channel $I_{KACh}$ is a heteromultimer of two inwardly rectifying $K^+$ channel proteins. *Nature* **374**:135-141.

Krapivinsky, G., Krapivinsky, L., Velimirovic, B., Wickman, K., Navarro, B., and Clapham, DE. 1995b. The Cardiac Inward Rectifier $K^+$ Channel Subunit, CIR, does not comprise the ATP-sensitive $K^+$ channel, $I_{KATP}$. *J. Biol. Chem.* **48**:28777-28779.

Kubo, Y., Baldwin, TJ., Jan, YN., and Jan, LY. 1993a. Primary structure and functional expression of a mouse inward rectifier potassium channel. *Nature* **362**:127-133.

Kubo, Y., Reuveny, E., Slesinger, PA., Jan, YN., and Jan, LY. 1993b. Primary structure and functional expression of a rat G-protein-coupled muscarinic potassium channel. *Nature* **364**:802-806.

Kubo, Y. 1996. Effects of extracellular cations and mutations in the pore region on the inward rectifier $K^+$ channel IRK1. *Recept. & Chann.* **4**:75-83.

Kunkel, MT., and Peralta, PG. 1995. Identification of domains conferring G protein regulation on inward rectifier potassium channels. *Cell* **83**:443-449.

Liman, ER., Tytgat, J., and Hess, P. 1992. Subunit stoichiometry of a mammalian $K^+$ channel determined by construction of multimeric cDNAs. *Neuron* **9**:861-871.

Lopatin, AN., Makhina, EN., Nichols, CG. 1994. Potassium channel block by cytoplasmic polyamines as the mechanism of intrinsic rectification. *Nature* **372**:366-369.

Lopatin, AN., and Nichols, CG. 1995. The mechanism of inward rectification of potassium channels. *J. Gen. Physiol.* **106**:923-955.

Lopatin, AN., and Nichols, CG. 1996. [$K^+$] dependence of polyamine-induced rectification in inward rectifier potassium channels (Irk1, Kir2.1). *J. Gen. Physiol.* **108**:105-113.

Lu, Z., and MacKinnon, R. 1994. Electrostatic tuning of $Mg^{2+}$ affinity in an inward rectifier $K^+$ channel. *Nature* **371**:243-246.

MacKinnon, R. 1995. Determination of the subunit stoichiometry of a voltage-activated potassium channel. *Nature* **350**:232-235.

Mazzanti, M., and DeFelice, LJ. 1988. K channel kinetics during the spontaneous heart beat in embryonic chick ventricle cells. *Biophys. J.* **54**:1139-1148.

Matsuda, H. 1991. Magnesium gating of the inwardly rectifying $K^+$ channel. *Annu. Rev. Physiol.* **53**:289-298.

Matsuda, H., Saigusa, A., and Irisawa, H. 1987. Ohmic conductance through the inwardly rectifying $K^+$ channel and blocking by internal $Mg^{2+}$. *Nature* **325**:156-159.

McPherson, CD., Pierce, GN., and Cole, WC. 1993. Ischemic cardioprotection by ATP-sensitive $K^+$ channels involves high-energy phosphate preservation. *Am. J. Phys.* **265**:H1809-1818.

Motulsky, HJ., and Ransnas, LA. 1987. Fitting curves to data using nonlinear regression: a practical and nonmathematical review. *FASEB J.* 1:365-374.

Nichols, CG., and Lopatin, AN. 1997. Inward Rectifier Potassium Channels. *Annu. Rev. Physiol.* **59**:171-191

Noda, M., Shimizu, S., Tanabe, T., Takai, T., Kayano, T., Ikeda, T., Takahashi, H., Nakayama, H., Kanaoka, Y., Minamino, N., *et al.*. 1984. Primary structure of *Electrophorus electricus* sodium channel deduced from cDNA sequence. *Nature* **312**:121-127

Noma, A. 1983. ATP-regulated $K^+$ channels in cardiac muscle. *Nature* **305**:147-148.

Pongs, O. 1993. Structure-function studies on the pore of potassium channels. *J. Membr. Biol.* **14**:320-323.

Rudy, B., and Iverson, LE. 1993. Expression of Ion Channels in *Xenopus* oocytes. In: *Methods in Enzymology Volume 207 Ion Channels.* ed. Rudy, B., and Iverson, LE. pp225-238.

Sakmann, B., and Trube, G. 1984. Conductance properties of single inwardly rectifying potassium channels in ventricular cells from guinea-pig heart. *J. Physiol.* **347**:641-657.

Sherman-Gold, R. 1993. Advanced methods in electrophysiology. In: *The Axon Guide for Electrophysiology & Biophysics Laboratory Techniques.* ed. Sherman-Gold, R. pp91-94.

Shimoni, Y., Clark, RB., and Giles, WR. 1992. Role of an inwardly rectifying potassium current in rabbit ventricular action potential. *J. Physiol.* **448**:709-727.

Slesinger, PA., Patil, N., Liao, J., Jan, YN., and Jan, LY. 1996. Functional effects of the mouse *weaver* mutation on G protein-gated inwardly rectifying potassium channels. *Neuron* **16**:321-331.

Stanfield, PR., Davies, NW., Shelton, PA., Sutcliffe, MJ., Khan, IA., Brammar, WJ., and Conley, EC. 1994. A single aspartate residue is involved in both intrinsic gating and blockage by $Mg^{2+}$ of the inward rectifier, IRK1. *J. Physiol (Lond)* **478**:1-6.

Stevens, EB., Woodward, R., Ho, I., and Murrell-Lagnado, R. 1997. Identification of regions that regulate the expression and activity of G protein-gated inward rectifier $K^+$ channels in *Xenopus* oocytes. *J. of Physiol.* **503.3**:547-562.

Taglialatela, M., Ficker, E., Wible, B., and Brown, AM. 1995. C-terminus determinants for $Mg^{2+}$ and polyamine block of the inward rectifier $K^+$ channel IRK1. *EMBO J.* **14**:5532-5541.

Tanabe, T., Takeshima, H., Mikami, A., Flockerzi, V., Takahashi, H., Kangawa, K., Kojuma, M., Matsuo, H., Hirose, T., and Numa, S. 1987. Primary structure of the receptor for calcium channel blockers from skeletal muscle. *Nature* **328**:313-318.

Tinker, A., Jan, YN., and Jan, LY. 1996. Regions Responsible for the Assembly of Inwardly Rectifying Potassium Channels. *Cell* **87**:857-868.

Tucker, SJ., Bond, CT., Herson, P., Pessian, M., and Adelman, JP. 1996. Inhibitory interactions between two inward rectifier $K^+$ channel subunits mediated by the transmembrane domains. *J. of Biol. Chem.* **271**:5866-5870.

Tygat, J., Buyse, G., Eggermont, J., Droogmans, G., Nilius, G., and Daenens, P. 1996. Do voltage-gated Kv1.1 and inward rectifier Kir2.1 potassium channels form heteromultimers? *FEBS Lett.* **390**:280-284.

Vandenberg, CA. 1987. Inward rectification of a potassium channel in cardiac ventricular cells depends on internal magnesium ions. *Proc. Natl. Acad. Sci. U.S.A.* **84**:2560-2564

Vandenberg, CA. 1995. Chapter 8: Cardiac Inward Rectifier Potassium Channel. In *Ion Channels in the Cardiovascular System.* Spooner, PM., and Brown, AM., eds. New York, NY. Futura Publishing Co. pp145-167.

Wible, BA., Taglialatela, M., Ficker, E., and Brown, AM. 1994 Gating of inwardly rectifying $K^+$ channels localized to a single negatively charged residue. *Nature* **371**:246-249.

Yang, J., Jan, YN., and Jan, LY. 1995. Determination of the Subunit Stoichiometry of an Inwardly Rectifying Potassium Channel. *Neuron* **15**:1441-1447.

Yang, J., Yu, M., Jan, YN., and Jan, LY. 1997. Stabilization of ion selectivity filter by pore loop ion pairs in an inwardly rectifying potassium channel. *Proc. Natl. Acad. Sci. U.S.A.* **94**:1568-1572.

# IMAGE EVALUATION TEST TARGET (QA-3)

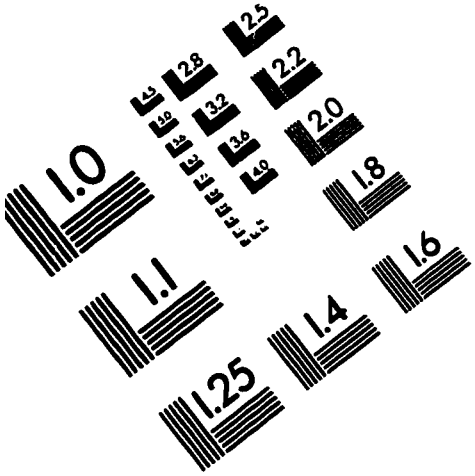


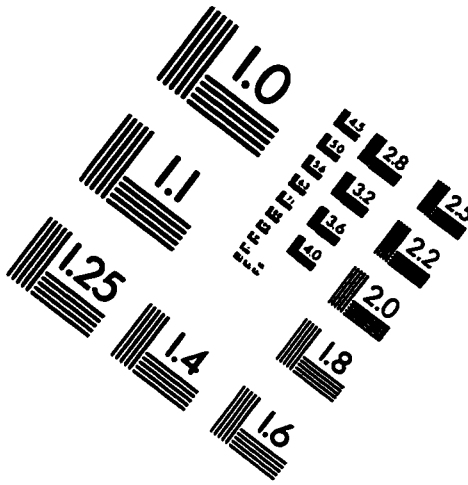


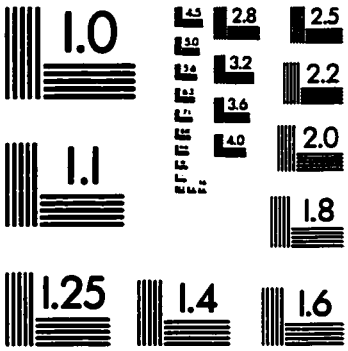


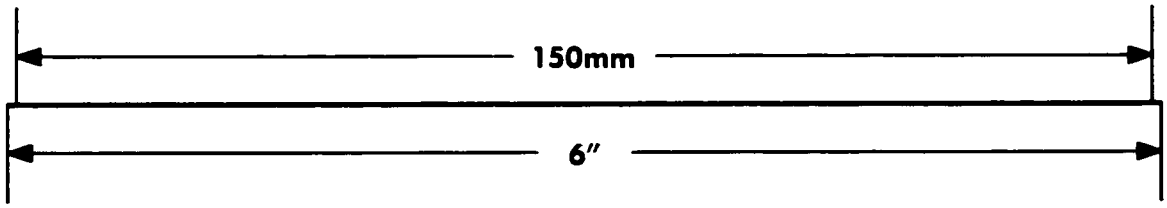


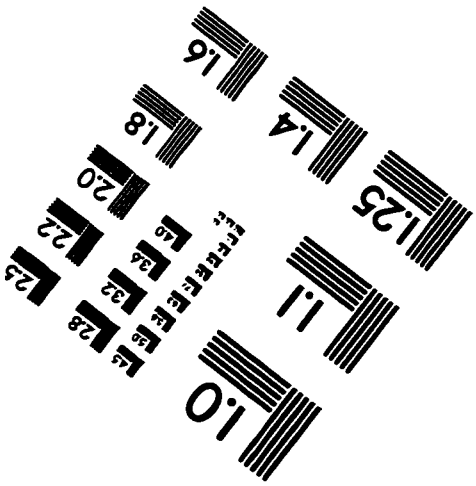


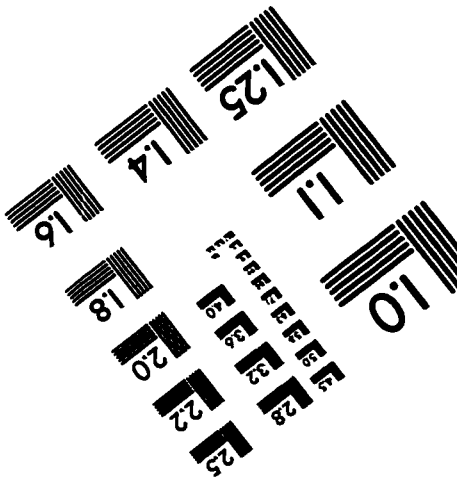


APPLIED IMAGE, Inc
1653 East Main Street
Rochester, NY 14609 USA
Phone: 716/482-0300
Fax: 716/288-5989